Aus dem Deutschen Herzzentrum Berlin
Klinik für Innere Medizin/Kardiologie

DISSERTATION

# Techniques of Mapping and Isolation of the Pulmonary Veins in Patients with Atrial Fibrillation

zur Erlangung des akademischen Grades
Doctor medicinae (Dr. med.)

vorgelegt der Medizinischen Fakultät
Charité – Universitätsmedizin Berlin

von

Chen, Xiao-Ming

aus Guangzhou, VR China

Gutachter/in: 1. Prof.Dr. med. E. Fleck

2. Prof.Dr. med.J. MüllerßEhmsen

3. Prof.Dr. H.-J. Trappe

Datum der Promotion: .23.06.2013

# Abstract


## Title: Techniques of Mapping and Pulmonary Vein Isolation in Patients with Atrial Fibrillation

Chen, Xiao-Ming

## Background

Electrical isolation of the pulmonary veins (PVs) is now the cornerstone of the ablative treatment of atrial fibrillation (AF). Traditional catheter ablation that applies the “point-by-point” approach guided by a three-dimensional imaging system is technically complex and time-consuming. Thus, there is a continuing search for alternative methods for ablation and imaging that should be as effective but more easily with shorter procedure times and a reduced complexity of the procedure. Cryoballoon with a micromapping catheter inserted through the central lumen, pulmonary vein ablation catheter (PVAC®), the high-density mesh ablation catheter (MESH) are widespread used but never underwent a direct comparison regarding efficacy; three-dimensional rotational angiography or atriography (3D-ATG) is the new electrophysiologic (EP) imaging technique which combines the accuracy of direct angiography with the benefits of computer animation.

## Objective

The purpose of this study was to: (1) assess the efficacy and safety of the new ablation catheters such as novel cryoballoon catheter, PVAC, and the MESH catheter compared with the conventional point-by-point RF ablation catheter; (2) compare the procedural and clinical outcome of catheter ablation for AF using either three-dimensional electroanatomical mapping (CARTO) or 3D-ATG.

## Methods

(1) From January 2008 to July 2010, 176 consecutive patients with symptomatic AF (mean age 61±11 years, 67.0% paroxysmal AF, 33.0% persistent AF) were divided to ablation using simplified cryoballoon catheter (52 patients), PVAC (46 patients), the MESH catheter (26 patients), and open-irrigation RF ablation catheter (52 patients).

(2) From January 2007 to December 2008, 134 consecutive patients with symptomatic AF (mean age 59±11 years, 56.7% paroxysmal AF, 43.3% persistent AF) were randomized to ablation using either 3D-ATG (66 patients) or CARTO (68 patients).

## Results

(1) There were no significant differences of complete PV isolation (71.2% of cryoballoon, 76.1% of PVAC, 65.4% of MESH, and 76.9% of RF, respectively, $P>0.05$) and successful isolation of targeted PVs (88.5% of Cryoballoon, 95.1% of PVAC, 90.4% of MESH, and 91.8% of RF, respectively, $P>0.05$) among the four groups. Procedure time was lowest in the PVAC group ($P<0.001$); fluoroscopy time was lowest in the MESH group ($P<0.001$). One patient had phrenic nerve palsy in the cryoballoon group, one case of air embolism was observed in the PVAC group, and one Tamponade was observed in the MESH group. There were no significant differences of complication rate among the four groups. After a mean follow-up of 11±8 months, there was no significant difference in clinical outcome among the four groups concerning AF recurrence ($P=0.25$).

(2) Procedure time, fluoroscopy time, RF ablation time, radiation exposure was shorter in the 3D-ATG group: 185.1±35.0 minutes versus. 233.1±50.8 minutes, $P<0.001$; 44.0±13.0 minutes vs. 57.1±29.2 minutes, $P<0.001$; 34.3±15.2 minutes vs. 47.0±17.9 minutes; $P<0.001$; 155417.2±80487.9 mGy $cm^2$ vs. 223409.0±144649.1 mGy $cm^2$, $P=0.001$; respectively. There were no major complications. After a mean follow-up of 14±13 months, there was no significant difference in clinical outcome using either 3D-ATG or CARTO concerning the AF recurrence (59.1% vs. 58.8%, $P=0.784$).

## Conclusions

(1) Simplified cryoballoon, PVAC, and the MESH catheter all represent safe, efficacious alternative for PV isolation. They all reduce both procedure and fluoroscopy time and make the procedure simple. The short- and middle-term efficacy of these catheters is comparable to a conventional point-by-point ablation technique.

(2) Three-dimensional ATG allows AF ablation to be guided with lower radiation exposure, shorter procedure time and similar outcome compared with CARTO. The ease of use and accurate 3D representation of the LA anatomy make 3D-ATG a reasonable alternative to conventional 3D electroanatomic mapping systems, however, without advanced mapping functions.

## Keywords

Pulmonary vein isolation; Catheter ablation; Atrial fibrillation; Rotational angiography; Atriography; 3D electroanatomical systems; Imaging

# Techniques of Mapping and Pulmonary Vein Isolation in Patients with Atrial Fibrillation

# Techniques of Mapping and Pulmonary Vein Isolation in Patients with Atrial Fibrillation

## 1. Introduction

Atrial fibrillation (AF) is the most common supraventricular tachyarrhythmia encountered in clinical practice and a leading cause of morbidity and mortality. It is independently associated with increased risk of a variety of adverse outcomes, including thromboembolic complications such as stroke, heart failure, mortality, and hospitalization, and it also impairs quality of life. It can be defined as paroxysmal, persistent, or permanent [1]:

Paroxysmal AF. Episodes of AF which do not last longer than 7 days and terminate spontaneously.

Persistent AF. The episodes of AF last longer than in paroxysmal AF (from 7 days up to several months) and do not terminate spontaneously. Pharmacological or electrical cardioversion is necessary for termination. After cardioversion, sinus rhythm can be maintained for several days to months.

Permanent (chronic) AF. AF is present for several months to years and neither pharmacological nor electrical cardioversion is successful anymore (immediate relapse or primary failure).

Approaches to the management of AF include rate or rhythm control. Rate control can be achieved by slowing the ventricular response rate with pharmacological agents or ablation of the atrioventricular (AV) node coupled with ventricular pacing. Rhythm control can be attempted pharmacologically with antiarrhythmic medications, with or without electrical cardioversion; surgically via the maze procedure; or more recently, utilizing catheter ablation of atrial tissue to restore sinus rhythm. Both rate and rhythm control strategies necessitate the use of anticoagulation to reduce the incidence of thromboembolic stroke. [2]

Large randomized trials have failed to demonstrate an improvement for mortality of the pharmacological rhythm control strategy as compared with the rate control strategy, indicating that rate control may be an adequate treatment for AF. However, further study determined that

the presence of AF at the time of study termination was a more potent predictor of mortality than the treatment strategy, suggesting the importance of sinus rhythm [3].

The exact mechanisms underlying AF are still poorly understood despite many years of research and speculation. Since the description of the multiple wavelet hypothesis by Moe and Abildskov [4], it has become generally accepted that AF is the result of the random propagation of multiple wavelets across the atria, a process that is independent of the initiating event.

Although many aspects of origin and perpetuation of AF are still unknown, the general concept of Haissaguerre assuming a fundamental role of the pulmonary vein (PV) stands beyond discussion. [5] Consequently, electrical isolation of the PVs from the left atrium (LA) has become the cornerstone of most of the various techniques used for catheter ablation of atrial fibrillation [6, 7]. Also the generally accepted endpoint of the procedure is the demonstration of a complete block between the LA and the PVs [8, 9]. The most recent European guidelines have now suggested that ablation might be offered as first-line therapy in selected patients with symptomatic paroxysmal or persistent AF, refractory to at least one antiarrhythmic drug [10-12], even prior to antiarrhythmic drugs in selected patients with highly symptomatic paroxysmal AF and no significant structural heart disease as a Class IIb recommendation[11].

Radio-frequency ablation of atrial tissue by application of energy through intracardiac catheters has become a major therapeutic method for AF [13, 14], and there is significant clinical evidence that the PV region and the posterior LA are crucial for maintenance of AF in paroxysmal AF patients [13]. The RF ablation procedure consists of generating electrical barriers in various sites of the atria by altering the tissue properties in the vicinity of the ablating catheter tip. The extent of the altered tissue depends on the power and duration of the application as well as on the characteristics of the tissue itself.

It has been about 17 years since the first serious attempt to perform catheter ablation to cure AF [15]. Shortly after Swartz et al. introduced the catheter-based maze procedure [15], Haissaguerre and colleagues published a landmark paper revealing that the PVs are an important source of triggering foci for paroxysmal AF [16]. This discovery caused electrophysiologists to focus on PVs as important target sites for AF ablation, marking a new era in the treatment of AF [5].

Various techniques were utilized to achieve electrical isolation of the PVs (PVI) including:

(1) segmental isolation introduced by Haissaguerre and colleagues [17]; (2) PVI at the antrum of the PVs at the atrium-venous junction using intracardiac ultrasound guidance or electroanatomical mapping [18] [19]; and (3) circumferential PV ablation popularized by Pappone et al [20].

## 1.1 Ablation techniques

The lack of a clear mechanistic understanding of AF is reflected in the pattern of development of multiple different technologies for its cure. However, consensus exists now that pulmonary vein isolation, preferably at an antral level, should be the cornerstone of any atrial fibrillation ablation procedure. The primary purpose of lesion-forming technologies in AF is to create safe and effective myocardial lesions in a reasonable time frame while avoiding collateral damage. The complex anatomy of the left atrium creates unique difficulties for any lesion-forming technology employed in the ablation of AF. Unfortunately, the ideal energy source for the treatment of AF has yet to be developed, and thus multiple different technologies are still used. Lesion-forming technologies currently employed in the treatment of AF include radio-frequency (RF) energy, cryothermal energy, and lasso-balloon.

The initial procedures developed for pulmonary vein isolation (PVI) utilized standard 4-mm tip RF catheters. Subsequently, cooled-tip RF and balloon-based technologies (to approximate the pulmonary vein atrial junction) have been more recently developed.

### 1.1.1 Point-by-point radio-frequency ablation

The technique as originally described utilizes one circumferential mapping catheter placed within the PVs and another ablation catheter in the LA sequentially targeting earliest activation from the LA into the PVs [17]. Two variants of PVI are practiced [21]]: circumferential PV ablation (CPVA) which relies on the anatomical creation of a complete isolation barrier and the segmental technique or its variants which depend upon electrical activation to pinpoint the precise input(s) and perform targeted ablation. Both techniques as currently practiced required appropriate and stable positioning of two catheters: one to ablate and the other to map and verify isolation. Both techniques are complex and time consuming including the time taken for

each individual ablation, the time to search for the next input/next site and the stabilization of catheters before delivering RF energy, and require a high degree of operator skill.

RF energy was one of the earliest energy sources used for catheter ablation and is the energy source that has been most extensively studied. In general, there are two types of irrigated catheters for the ablation of AF. The first is closed-loop irrigation catheters, which have an internal thermocouple and continuously circulate saline within the electrode tip, internally cooling the tip. The second type of irrigated catheter is open irrigation catheters, which have an internal thermocouple and multiple irrigation holes located around the electrode, through which saline is continuously flushed, providing both internal and external cooling.

Focal point-by-point RF ablation has shown considerable success in treating paroxysmal AF. However, the risk of major complication is high. A major complication is generally defined as a complication that results in a permanent injury, prolongation of hospitalization, requirement of invasive intervention for treatment, or death [22]. Cappato et al published data from a worldwide survey investigating the methods, safety, and efficacy of catheter ablation procedures and reported an overall incidence of major complications of 4.5% and fatal outcomes in 0.15% of a total of 16,309 patients [23]. Other studies reported a major complication rate at 3.9%-5% [22]. Major complications include: (1) cardiac tamponade due to perforation (1.3%); (2) cardiac perforation; (3) direct injury to the phrenic nerve (0~11%); (4) esophageal injury which has been reported in approximately 10% of patients; (5) atrioesophageal fistulas (0.04%) which are rare but can be devastating and even lethal; (6) cerebrovascular thromboembolism which has been reported to occur in up to 2% of patients; (7) pulmonary vein stenosis which is a late complication reported in 0% to 10% (it is defined as mild if narrowed by <50%, moderate if narrowed by 50% to 70%, and severe if the narrowing is more than 70%); (8) iatrogenic atypical flutter (1.8%~14.3%); (9) vascular access complications including hematoma, femoral pseudo-aneurysm, and arteriovenous fistula; (10) other complications such as pyloric spasm and gastroparesis, etc. [22][24]

Furthermore, the procedure is complex, time consuming, and highly dependent on operator competency given the difficulties associated with creating contiguous curvilinear lesions with focal ablation. Thus, there is a continuing search for alternative methods that should be as effective but more easily performed with shorter procedure times and reduced complexity of the

procedure. Consequently, various models of single catheter devices are under investigation. Three of the newer devices, cryoballoon, PVAC, and MESH, are widespread used but have not yet undergone a direct comparison regarding efficacy.

### 1.1.2 Cryoablation balloon

Balloon-based catheter systems using various energy sources (cryothermal energy, non-focused ultrasound, highly focused ultrasound, laser, and radio-frequency) have been developed or are currently under investigation [25]. They potentially offer a simpler and faster means of achieving PV isolation that, theoretically, is less reliant on operator dexterity [26]. With regard to safety aspects, cryothermal energy may have advantages over other energy sources since both human and experimental animal data have demonstrated that the risk for PV stenosis[27], atrio-esophageal fistulae [28], and thrombus formation [29] is extremely low to absent with application of cryothermal energy.

#### 1.1.2.1 Tranditional cryoballoon technique

The cryoballoon technology (Arctic Front®, Cryocath Inc. Montreal, Canada) is currently available in two balloon sizes: 23mm and 28mm, but the 28mm balloon is extensively used at present because the larger balloon results in isolation at a more antral level and is less likely to injure the phrenic nerve [30]. Using a simple over-the-wire technique in conjunction with a steerable sheath, the balloon can be navigated to each PV ostium. After demonstrating balloon occlusion of the PV through PV angiography and thereby confirming sufficient balloon-wall contact, cryothermal energy is applied by injection of the refrigerant $N_2O$ into the balloon.

This novel catheter designs that deliver circumferential ablation centered on PV ostia have the potential to reduce procedural times and complexity while delivering at least comparable clinical outcomes. One such technology, the cryoablation balloon, has been in use in Europe since 2005 and received U.S.Food and Drug Administration approval in 2010 for ablation of paroxysmal atrial fibrillation (PAF) [31]. As an energy source for LA ablation, cryotherapy offers several potential advantages over radio-frequency ablation. In experimental models, it creates cellular disruption without altering target tissue architecture and is less thrombogenic [29]. This

could reduce procedural complications such as PV stenosis, atrioesophageal fistulation, and thromboembolism [30] [32] [33]. Catheter stability provided by tissue adherence during cryoballoon can be helpful at sites where good catheter-tissue contact may be difficult to maintain.

However, a second transseptal puncture is a common approach for insertion of a diagnostic spiral catheter to evaluate PV isolation after each cryoenergy application. Likewise, when utilizing a single transseptal LA access, the cryoballoon must first be removed to assess PV isolation by placing a "lasso" catheter in the vein ostium post cryo application. Frequent exchanges increase the risk of air embolism and/or damage to the balloon catheter itself. In addition, by removing the balloon, a difficult to obtain occlusion position is often lost and difficult to regain should additional cryo application(s) become necessary. Currently, the operator has no "real time" means to assess the effect of cryoballoon ablation on PV conduction during the freezing period [34].

#### 1.1.2.2 Simplified cryoballoon technique

As the conventional cryoballoon technique requires two transseptal punctures, one to accommodate the balloon and the other for the PV circular mapping catheter, a single transseptal puncture can also be effective in which the operator interchanges the cryoballoon catheter and mapping catheter to verify whether the target PV has been isolated. Neither of these techniques is ideal and, thus, a technique that facilitates simultaneous PV potential mapping during and immediately following cryoballoon without repositioning of the balloon is needed. In response to this limitation, we proposed to first introduce a mapping catheter through the cryoballoon catheter's central lumen. By combining the catheters in this way, the procedure can be successfully completed with just one transseptal puncture and without interchanging the catheters, and the technique is feasible and effective[35].

### 1.1.3 Pulmonary vein ablation catheter (PVAC®)

The pulmonary vein ablation catheter (PVAC®) (Medtronic, Medtronic, Minneapolis, MN, USA) is also a novel circular multi-electrode catheter that has been used in combination with a multichannel, duty-cycled radio-frequency generator (GENius, Medtronic, Minneapolis, MN,

USA) for mapping and ablation all through a single catheter. This multi-electrode over-the-wire device capable of circular mapping and RF energy delivery is intended to simplify the PV isolation procedure while reducing the risk of complications.

The first results using duty-cycled bipolar unipolar radio-frequency (PVAC®) in pulmonary vein isolation were published by Boersma et al [36]. They reported high efficacy in PV isolation in 98 patients predominantly with paroxysmal AF and impressively low procedural and fluoroscopy times. These results were then validated in recent years [37]-[40].

### 1.1.4 MESH

The high-density mesh ablation catheter (MESH, Bard Electrophysiology, Lowell, MA, USA) is an expandable mesh electrode and can be used for both electrogram recording and the delivery of pulsed radio-frequency RF energy in a circular fashion at the ostium of PVs [41]. It is a 36 pole high-density mapping and ablation catheter that has a braided, expandable mesh electrode configuration mounted onto a nonsteerable 8F shaft, which can be spanned as an umbrella with a maximum equatorial diameter of 30mm. When placed in the antrum, its position is stable during the ablation procedure. The MESH consists of 36 wires that can be used to record 36 unipolar or bipolar electrograms. The MESH delivers pulsed RF energy via the Tempulse Pulsed RF Controller (Bard Electrophysiology), a device that accepts unmodulated power from a compatible radio-frequency lesion generator as input. In the experimental preclinical canine study, it has been proved to be an efficacious, safe, and reliable technology to obtain PV isolation [42]. Several clinical studies have also showed that this method is safe and proved to be efficient in obtaining acute pulmonary vein isolation but it yields a high AF recurrence rate at long-term follow-up even after a second procedure with the same tool[43]-[46].

## 1. 2. Imaging techniques

Because of the complexity and the multitude of mechanisms that play a role in the genesis of AF, catheter ablation often requires complex lesion sets in the atrium and a three-dimensional (3D) perspective of the left atrium may be particularly helpful. Therefore, there has been much

emphasis on imaging of the heart, specifically the left atrium, to facilitate catheter ablation. Imaging provides (1) identification of the number, location, and size of the pulmonary veins and their ostia; (2) a three-dimensional (3D) perspective of the left atrial geometry and anatomical landmarks; (3) the ability to create complex circular or linear ablation lines; (4) identification of the location, proximity, and size of critically important adjacent structures such as the esophagus; (5) a guide for transseptal puncture; (6) less reliance on fluoroscopy, with a decrease in radiation exposure for both the patient and the operator [47].

The conventional mapping technique-fluoroscopy-has great merits in the development of clinical electrophysiology and it has helped a great deal in the understanding of mechanisms of initiation and sustenance of clinical arrhythmias and in their RF ablation. It has been the time-honored, primary imaging modality for catheter ablation of AF. It is readily available and provides real-time imaging. However, even when biplane fluoroscopy is used, a 3D appreciation of the left atrial geometry is difficult. Fluoroscopy results in cumulative radiation exposure for both the patient and the operator, which can be substantial when the duration and number of procedures performed, are considered [47]. Therefore, the traditional two-dimensional imaging methods such as fluoroscopy do not satisfy the needs of complex catheter navigation inside three-dimensional anatomic structures that may not be confined to the radiographic cardiac silhouette (e.g. PVs). Consequently, improved imaging modalities, with the goals of improving catheter positioning, knowledge of the true anatomy, and location of the lesion set, aim to make the AF ablation procedure easier, safer, and quicker to perform. A number of different imaging methods are now used, including fluoroscopy, potentially overlaid with a three-dimensional shell imported from cardiac computed tomography (CT) or cardiac magnetic resonance imaging (MRI), 3D electroanatomical systems, which again can be merged with a 3D shell from CT or MRI, intracardiac echocardiography, and 3D rotational atriography.

### 1.2.1 CARTO SYSTEM

The magnetic electroanatomical mapping system (or CARTO, Biosense-Webster Inc, Diamond Bar, CA) is a nonfluoroscopic mapping system that uses electromagnetic principles to accurately determine the location and orientation of the mapping and ablation catheter along

with simultaneous recording of local electrical signals (bipolar or unipolar local electrograms). Sequentially acquired information at multiple locations of the catheter within the heart chamber coupled with local electrograms enables reconstruction of the electroanatomic maps of the respective heart chamber. It is composed of an ultra-low magnetic field emitter (locator pad), a miniature passive magnetic field sensor embedded in the mapping and ablation catheter and a data processing unit with graphical display. The magnetic field emitter placed beneath the operating table at the level of the patient's chest generates an ultra-low magnetic field in the range of 0.05 to 0.2 Gauss. The magnetic field emitter consists of three coils generating a magnetic field that reduces in strength as a function of the distance from the coil. The sensor embedded in the mapping and ablation catheter senses the strength of magnetic fields produced by each coil enabling the determination of the distance from each coil. When the catheter tip moves in the magnetic field, the location sensors measure the strength of the field, thus enabling the determination of the distance from each of the coils. The distances are radii of theoretical spheres around each coil. The intersection of all three spheres defines the location of the sensor and, thus, of the mapping catheter tip in space [47].

The greatest advantage of electroanatomic mapping relies on its ability to integrate anatomic and electrophysiological information in the form of electroanatomic maps, so that it links origin of arrhythmia to discrete anatomic structures, for example, an activation map can be superimposed on the 3D anatomy, targeting the site where demonstrating complex fractionated atrial electrograms (CFAEs) during AF or facilitating diagnosis of atrial tachycardia. The second advantage has to do with its ability to visualize the ablation catheter, tag precisely the ablation sites, and renavigate the ablation catheter to the sites of prior current application or close to them. Third, with its capability to characterize normal and diseased tissue and thus the potential arrhythmogenic substrate, electroanatomic mapping has enabled ablation of hemodynamically unstable arrhythmias [48]. Also since contrast agents are not necessary for CARTO mapping, this method may be preferred for patients with severe heart failure, or liver and/or renal insufficiency.

### 1.2.2 EnSite NavX™ system

EnSite NavX™ (St. Jude Medical, Inc., Minneapolis MN) is another commonly used 3D mapping system which uses impedance sensing between an externally applied electrical field and standard customary catheter electrodes. The fundamental principle underlying EnSite NavX™ navigation is that of an impedance-based measure, which is dependent on the voltage gradient that exists across tissue when a current is applied through the surface electrodes. This mapping system is based on localization of multiple electrodes using an electrical field generated by three pairs of surface electrodes placed on the patient's body along three orthogonal axes (x, y, and z axes) [49]. The conventional catheters are localized by measuring the electrical potential or field strength received by the different frequencies from the x, y, and z axes emitted by the patches. The three-dimensional location of each catheter electrode is located by sensed voltage gradients in all the axes.

However, both these electroanatomic mapping techniques lack accuracy of reconstruction because they are based on indirect assumptions and cannot provide direct visualized images of the left atrium and the PVs.

### 1.2.3 Three-dimensional rotational atriography

Angiography has always been the gold standard of anatomic accuracy, but application of biplane angiography to real-time guidance of ablation procedures is limited. The latest development in electrophysiologic (EP) imaging is 3D rotational angiography or atriography (3D-RTA or 3D-ATG), which combines the accuracy of direct angiography with the benefits of computer animation. While pre-procedure CT/MRI images provide visualization of the left atrium and the PVs and facilitate integration with the electroanatomic mapping systems, a significant drawback is the time lag to the actual procedure. There may be temporal changes in the size and location of the anatomical structures between the time of image acquisition and ablation. This limitation can be overcome with the use of 3D-ATG in the EP laboratory for reconstruction of LA and PV as well as the surrounding structures such as the esophagus [50, 51]. The principle of 3D-ATG is similar to the CT scan where images acquired from different angles are reconstructed to generate a three-dimensional image. The C-arc X-ray system is rotated over

220° (from right anterior oblique 110° to left anterior oblique 110°) during the opacification of the PVs and LA with a contrast medium [52]. The 3D images of LA, PVs, esophagus and the other surrounding structures can be segmented and registered with fluoroscopy to serve as a roadmap for ablation [53]. Therefore, it provides direct visualization of cardiac structures, whereas electroanatomic methods require either operator imagination or confirmation via other imaging modalities, such as CT. The contrast can be injected either from the right atrium (RA) or from the common trunk of the pulmonary artery for indirect LA angiography or directly into the LA for direct LA angiography. Resultant 3D-ATG images provide great detail of the LA/PV anatomy but require a high-dose adenosine injection and deep sedation to stop the heart and prevent antegrade washout of contrast from PVs. However, a considerable number of 3D-ATG reconstructions are suboptimal [51]. This is partly attributable to heart movement during image acquisition and fast contrast washout. Two methods have recently been proposed for improvement of image acquisition. Adenosine-induced asystole has been recently proposed for improvement of image acquisition [55]. Another method is rapid ventricular pacing (RVP) for 6~8 seconds which reduces atrial output, thus allowing for more contrast fill in the LA chamber to enhance delineation for the LA-PV anatomy [56]. Both methods can acquire optimized LA reconstructed images which have good correlation in the PV ostial diameters and left atrial appendage (LAA) to CT imaging [57]. Another advantage of 3D-ATG is that it can be performed during the ablation procedure, providing realistic anatomic detail at the time of the intervention.

Thus, rotational angiography has been proposed to facilitate 3D visualization of the anatomy and catheter manipulation. The advantage of this approach is that it can be performed in real time in the electrophysiology laboratory and may provide a more accurate assessment of the anatomy. However, further improvements in technology will be necessary to be able to record and tag catheter position on the 3D fluoroscopic image [36]. The accuracy of registration of 3D CT images with fluoroscopic projections was validated [56]. The study demonstrated that 3D-ATG could provide real-time images that were easily segmented and registered with excellent accuracy and concordance with live fluoroscopy and CT [53].

Larger clinical studies will be necessary to determine the utility of this technique during AF catheter ablation.

# 2. Objective

Electrical isolation of the PVs is the cornerstone of the ablative treatment of atrial fibrillation. New technologies may reduce the complexity of the procedure. The purpose of this study was to: (1) assess the efficacy and safety of the new ablation catheters such as the novel cryoballoon catheter, PVAC, and MESH catheter compared with the conventional point-by-point RF ablation catheter; (2) compare the procedural and clinical outcome of catheter ablation for AF using either three-dimensional electroanatomical mapping (CARTO) or 3D-ATG.

# Part I Comparison of efficacy and safety of catheter ablation for atrial fibrillation using simplified Cryoballoon catheter, PVAC, MESH catheter, and point-by-point radio-frequency ablation catheter

## 3. Methods

### 3.1 Patient selection

Patients with symptomatic, medically refractory AF registered for ablation between January 2008 and July 2010 at the German Heart Institute Berlin were recruited. All patients had either ECG documented paroxysmal AF (defined as self-terminating AF episodes lasting <7 days) or early persistent AF(defined as episodes of AF that lasted > 7 days, requiring direct current cardioversion to restore sinus rhythm and transition from a clinical pattern of paroxysmal AF in the past 12 months) and unsuccessful treatment with at least one antiarrhythmic drugs. No patient had undergone prior PV ablation. Study inclusion criteria included a history of symptomatic AF with a normal left ventricular ejection fraction evaluated by echocardiography. All patients were treated with only one of these four catheter ablation techniques: simplified cryoballoon catheter, PVAC, MESH catheter, and open-irrigation RF ablation catheter.

Transesophageal echocardiography was performed prior to the procedure to exclude left atrial thrombus. All patients signed informed consent, and the study was performed in accordance with the Institutional Research guidelines at the German Heart Institute Berlin.

### 3.2 Procedure

#### 3.2.1 Intra-procedure 3D-ATG and 3D reconstruction of LA and PVs

Procedures were performed under conscious sedation and analgesia with appropriate doses of propofol. Venous access was obtained through the femoral vein. A 2-polar catheter (Osypka) was placed at the right ventricular apex (RVA). A stable catheter position and a pacing threshold ≤1.5mA/1.0ms had to be achieved. A 10-polar catheter (Inquiry, St. Jude Medical, St Paul, MN,

USA) was introduced into the coronary sinus for stimulation of the LA. After performance of one or two (only for point-by-point ablation procedure) transseptal punctures, one or two sheaths (the first was a steerable sheath corresponding to the ablation catheter we used, the second an SL0 sheath) were introduced into the LA (one for the ablation catheter and the other for the lasso catheter using the point-by-point ablation technique). A 6 Fr 'pigtail' catheter was placed in the LA and connected to a power injector.

In all patients, imaging was performed using an X-ray FD10 flat detector system (Allura Xper, Philips Healthcare, Best, The Netherlands). Left atrial-pulmonary venous chamber isocentering was achieved as follows [51]: the fluoroscopic image was divided into four quadrants. The examining table was adjusted in a way that the distal end of the pigtail catheter was at the right upper quadrant but close to the center of the image (about one-third of the distance between the center and right superior angle of the fluoroscopy screen) in three projections: right oblique 55° and anterior-posterior and left oblique 55°. The right ventricle was rapidly paced (cycle length 300~330ms depending on the basic ventricular rate of the patient) for 6-8 seconds. Reliable capture was warranted with double the minimum pacing voltage and a blood pressure decrease below 50 mmHg. Sixty milliliters of diluted contrast medium (20ml/s, Ultravist, Bayer-Schering, Berlin, Germany) was injected into the isocentered LA 2 seconds after the initiation of the rapid ventricle pacing. After a delay of 1s, rotational X-ray image acquisition was started using a 220° rotation (from a right anterior oblique [RAO] 110° to a left anterior oblique [LAO] 110°) over 4s at a sampling rate of 30 frames/s. [32] Rotational angiography of LA was achieved.

Rotational runs were then automatically transferred to a standard 3D-ATG X-ray workstation (EP Navigator 2.2, Philips Inc.) for CT-like image reconstruction after acquisition of ATG. If necessary, segmentation was corrected manually by adding some strokes to the 3D reconstruction. The 3D volume data sets were automatically fused with the fluoroscopic image. Since 3D-ATG data sets and fluoroscopic imaging were acquired by the same C-arm system, registration alignment and overlay were automatically performed on the workstation. The software used in this study enabled 3D visualization of the LA surface as well as endoscopic views by using cutting levels that could be freely orientated in order to achieve optimal visualization of the different structures [58]. If necessary, manual readjustment of the registration

was performed according to identifiable anatomical reference points and catheter position. This was validated in three different projections (Fig.1).

### 3.2.2 Simplified cryoballoon technique

In view of the limitations of the conventional cryoballoon catheter, we introduced a novel cryoballoon catheter which needed only a single transseptal puncture (28-mm, Arctic Front, CryoCath Technologies, Montreal, Canada) [35]. A microcircular mapping catheter (6-polar or 10-polar) with a 0.035-inch shaft diameter (ProMAP, ProRhythm Inc., Ronkonkoma, NY, USA) was introduced into the PV through the central lumen of the cryoballoon catheter (Fig. 2[35]). In turn, the cryoballoon catheter was introduced into the LA via a 12F steerable sheath (FlexCath, CryoCath Technologies). In addition to its function as a recording device, the microcircular mapping catheter was also used as a 'guide-wire'. Using the 'over-the-wire' technique with the steerable sheath, the balloon was guided to each PV ostium (Fig.3).

Before the balloon was inflated, the mapping catheter was placed in the PV to record the PV potential. The cryoballoon was then inflated and advanced toward the PV ostium guided by the 3D-ATG live imaging.

Cryoballoon catheter ablation was initiated with the freezing cycle set at 300 seconds. Internal proximal balloon temperature was continuously monitored. During the procedure, heparin boluses were repeatedly administered to maintain the activated clotting time between 250 and 300 seconds. When it was necessary, RVP was performed from the RVA at a cycle length of 300-330ms for 30 seconds at the beginning of cryoablation in order to improve local PV/balloon adhesion. The real-time recording of PV potentials' changes during the cryoablation procedure is shown in Fig. 4. After each ablation attempt, PV potentials were reevaluated with the mapping electrode at the same position. If the PV was not isolated, an additional application of cryothermal energy was made. The ablation endpoint was complete electrical isolation of all PVs.

During ablation of the right PVs, the decapolar catheter was withdrawn from the coronary sinus and repositioned in the superior vein cava to pace the phrenic nerve (cycle length 1200ms, 8-10mA/ 1.5ms). If the capture of phrenic nerve stimuli was lost, the ablation procedure was immediately stopped.

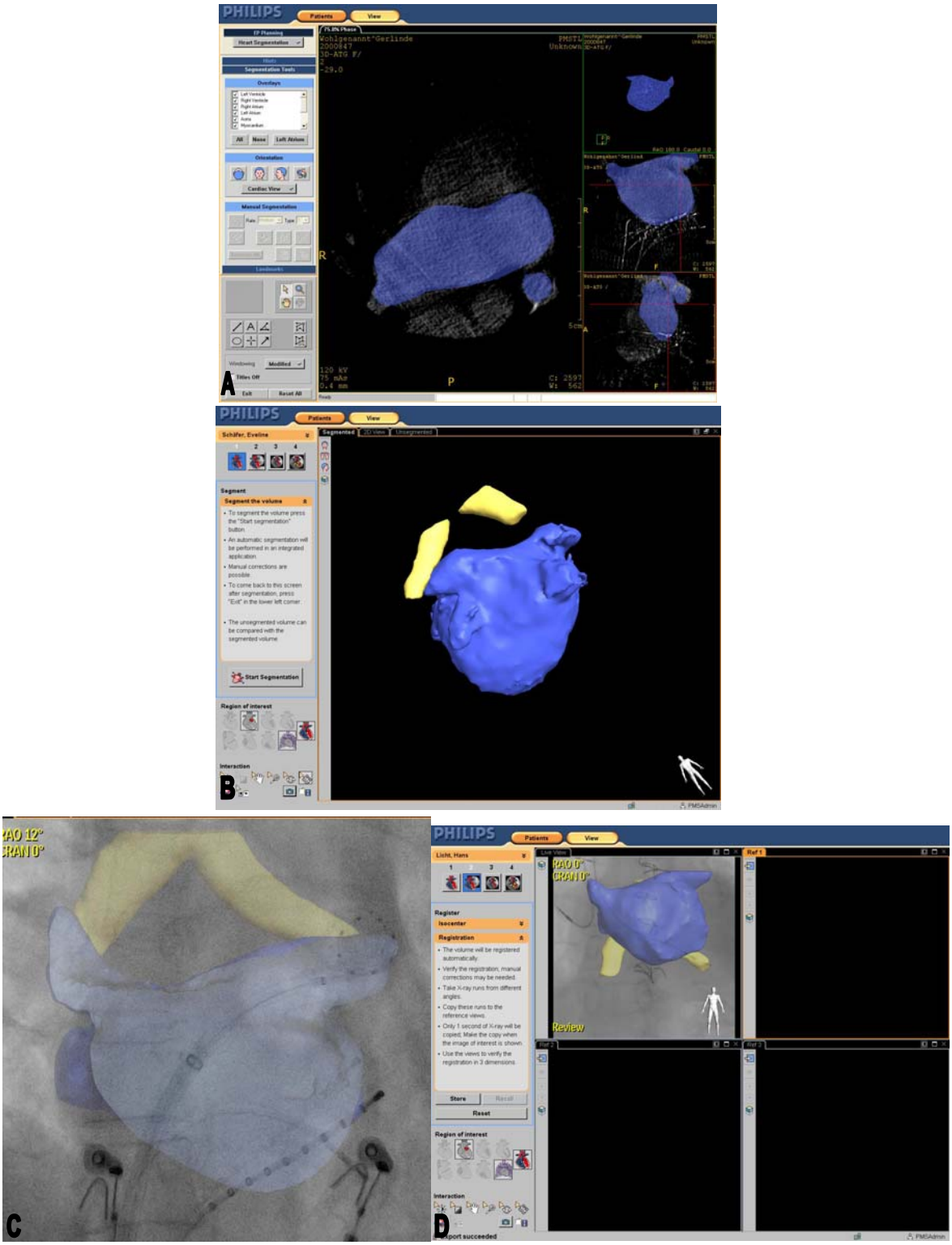


*Figure 1 (A) The segmentation window for the 3D reconstruction of LA and PVs. (B) 3D reconstruction of LA and PVs by 3D-ATG. Bronchi were colored yellow; (C) 3D-ATG image was overlaid on the fluoroscopy in the procedure of cryoballoon ablation. (D) Manual readjustment of the registration was performed when it was necessary and could be validated in three different projections (Ref1 toRef3).*

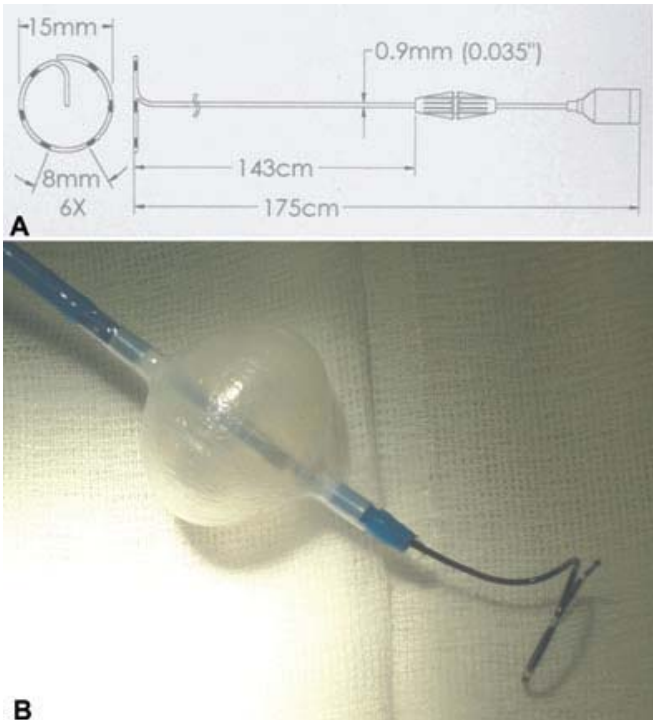


**Figure 2.** *The microcircular mapping catheter is a 6-pole or 10-pole circular catheter with a shaft diameter of only 0.035 inch and a circular ring diameter of 15mm. The mapping catheter can be introduced into the central lumen of the cryoballoon catheter and can be used as a "guide-wire" as well as a recording device. (A) Schematic representation of the mapping catheter. (B) Distal end of cryoballoon catheter equipped with the circular mapping catheter.*

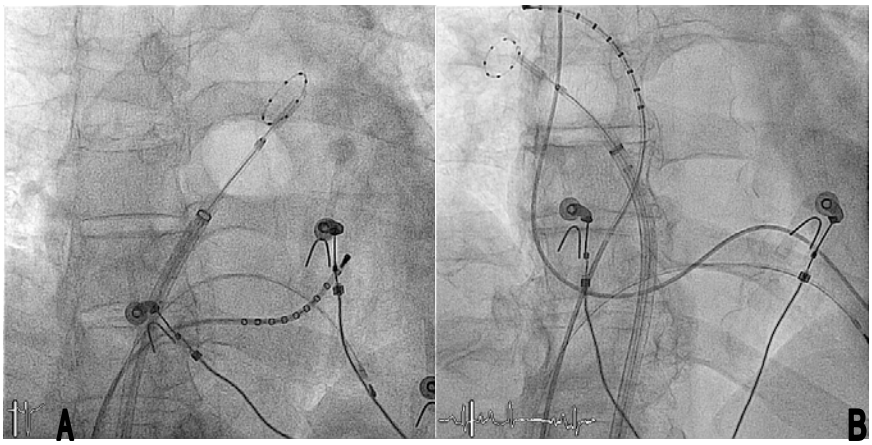


**Figure 3.** *Occlusion of the PVs with inflated cryoballoon in X-ray fluoroscopy. (A). Occlusion of the LSPV with inflated cryoballoon was in anterior-posterior projection. (B). Occlusion of the RSPV with cryoballoon catheter was in anterior-posterior projection. Decapolar catheter is placed in the superior vena cava.*

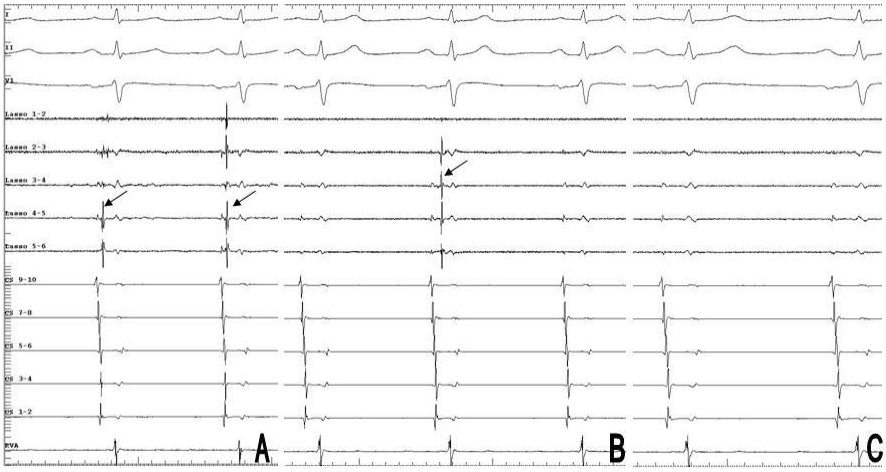


**Figure 4**. *Real-time recording of complete isolation of a left superior PV (LSPV) in sinus rhythm with the simplified cryoballoon technique. From top to bottom: surface ECG leads I, II, V1; endocardiograms in the 6-pole microcircular mapping catheter (lasso 1-2 to 5-6); endocardiograms in the coronary sinus (CS1-2 to 9-10); signals in the right ventricular apex (RVA). (100mm/s) (A)PV potentials (arrows) in the LSPV before ablation. (B) Progressive organization of activity and partial entrance block (2:1 block) in the LSPV during ablation (arrow). (C) Complete isolation of the LSPV.*

### 3.2.3 Pulmonary vein ablation catheter, ablation generator, and selectable energy modes

The PVAC is a 9 Fr, over-the-wire, circular, and decapolar mapping and ablation catheter with an adjustable 25mm helical electrode array comprising 3mm platinum electrodes with 3mm spacing (Fig. 5A). Catheter navigation and positioning are supported by both bidirectional steering and over-the-wire tracking. The electrode array can be extended to assume a spiral configuration that allows for various tissue contact positions. By rotating the catheter shaft with the distal tip engaged against anatomical structures, the diameter of the array could be effectively increased or decreased from 20mm to 35mm. By decreasing the array diameter with clockwise rotation, electrograms could be recorded and analyzed from inside the PV ostium. Counterclockwise rotation will increase the array diameter, facilitating mapping and ablation around the antrum of veins with larger diameters. The PVAC is positioned in the antral region of the targeted PV over a 0.032” guide-wire, which is selectively placed into different side branches of the PV to improve the tissue-electrode interface around the pulmonary vein

circumference [37] (Fig. 6).

The GENius™ generator (Fig.5B, 5C) is a multichannel RF generator capable of simultaneously delivering duty-cycled energy to operator-selected electrodes. The generator has 5 preset energy settings: bipolar, unipolar, and 3 ratios of bipolar-to-unipolar energy: 4:1 (80% bipolar and 20% unipolar), 2:1 (66.7% bipolar and 33.3% unipolar), and 1:1 (50% bipolar and 50% unipolar). Unipolar energy is defined as current flowing between a catheter electrode and the indifferent return electrode, whereas bipolar energy is current flow between adjacent electrodes. The mode defines the duration of RF delivery in bipolar or unipolar flow. When 1:1, 2:1, or 4:1 modes are selected, RF energy flows concurrently in both the bipolar and the unipolar fashion. Prior to ablation, the operator selects a target temperature, ablation duration, and bipolar-unipolar energy mode. During RF application, the generator modulates energy delivery in a temperature-controlled manner to reach the target temperature, with a maximum power of 10W per electrode. The display shows the temperature and power delivery for individual electrodes. Preclinical studies have shown that lesion depth is greater with the RF modes that have more unipolar component [59]. Specifically, the 4:1 mode of RF application has been shown to create a lesion that is approximately 3mm in depth (manufacturer's data). Increasing the amount of unipolar energy to the 2:1 mode adds approximately 1mm in depth.


**Figure 5.** *(A) Ablation frontiers (PVAC): Pulmonary vein ablation catheter, (B) GENius ™ multi-channel RF generator, and (C) GENius ™ remote control for generator.*

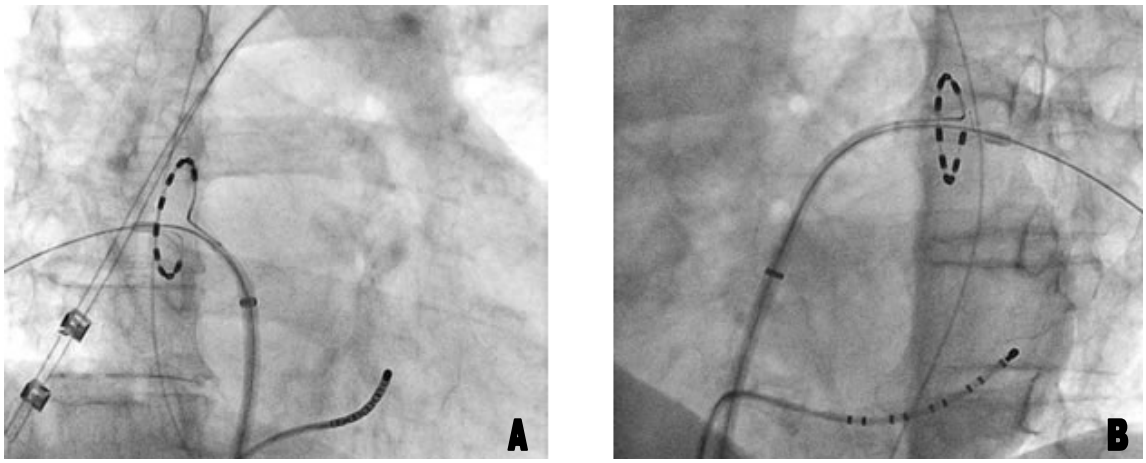


**Figure 6**. *PVAC was positioned in the targeted pulmonary vein in X-ray fluoroscopy: (A) RAO10°, (B) LAO60°*

***Mapping and ablation protocol***

The PVAC was deployed in the LA over a 0.032" guide wire inside the PV and then advanced until it was in close contact to the antral region proximal to the ostium. Stimulation was performed from different left atrial regions (distal coronary sinus and LA appendage, posterior LA) for the detection of PV potentials originating from the left- and right-side pulmonary veins, respectively. If no PV potentials were detected with the PVAC in the antral region, the catheter was further advanced into the PV ostium or inside the vein. All veins showing PV potentials spontaneously or as a result of pacing were targeted for antral ablation to achieve PV isolation. An optimal position for ablation was based on electrograms, with the goal of ablating local antral potentials of high amplitude on as many electrodes as possible for each application, and simultaneously guided by 3D-ATG live images (Fig. 7, Fig. 8). Care was taken to avoid energy application inside the PVs [59].

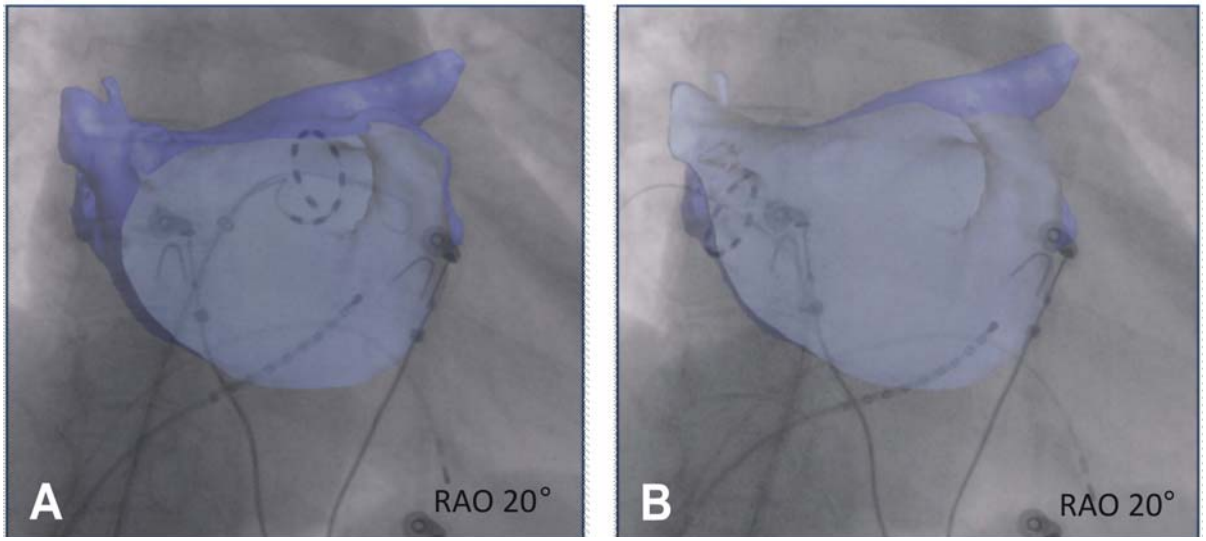


**Figure 7.** *3D-ATG navigation of PVAC procedure (A. LIPV, B. RIPV)*

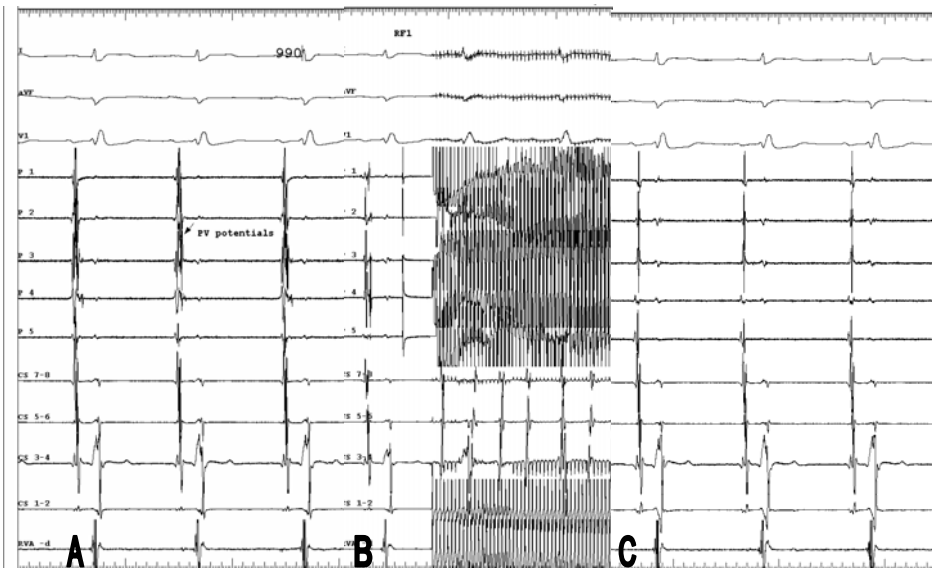


**Figure 8**. *Complete isolation of a left superior PV (LSPV) in sinus rhythm with the PVAC technique. From top to bottom: surface ECG leads I, aVF, V1; endocardiograms in the multielectrode PVAC catheter (P1-5); endocardiograms in the coronary sinus (CS 1-2 to 7-8); signals in the right ventricular apex (RVA).(50mm/s) (A) The activity of PV potentials in the LSPV before ablation. (B) Procedure of ablation using PVAC. (C) Complete isolation of the LSPV after PVAC ablation.*

### 3.2.4 MESH catheter

The high density mesh ablation system (Bard Electrophysiology, Lowell, MA, USA) consists

of an 8-Fr nonsteerable expandable catheter (30mm in diameter) designed to perform high-density 36-bipole mapping and RF energy delivery, a RF generator, and a TemPulse RF controller (Bard Electrophysiology, Lowell, MA, USA) (Fig. 9). The mesh electrode is constructed of two opposing 18-electrode interwoven helices that can be used to record 36 unipolar or bipolar electrograms or to deliver pulsed RF energy. In total, 36 unipolar or bipolar electrograms can be recorded simultaneously. Four thermocouples divide the circumference of the catheter into four quadrants allowing RF delivery in a temperature controlled mode.

After transseptal access was obtained, the catheter was advanced and deployed at the ostium of the targeted vein via an 11-Fr steerable transseptal sheath (Bard). A bolus of 5,000~8,000 IU (IU= international units) heparin (body weight adjusted) was administered intravenously followed by several boli of heparin to maintain an activated clotting time between 250 and 300 seconds. The retraction of a central wire allows the deployment of the catheter to a maximal diameter of 30mm. The position of the MESH catheter in relation to the PV ostium was determined by fluoroscopy (Fig. 10a) and 3D-ATG live image (Fig. 10b) and confirmed by intracardiac electrograms (Fig. 11). The MESH catheter was expanded in the distal part of each PV to assess the anatomy and the electrophysiological properties. If no electrical activity could be recorded, the catheter was retracted slowly until PV signals alone, atrial signals followed by PV signals, or atrial signals alone were observed.

Pulsed RF energy from a 100W RF generator (Stockert, Biosense Webster) is transferred to the TemPulse (Bard Electrophysiology) (Fig. 12), where the energy is multiplexed into 5ms pulses and delivered through half of the electrodes (every other wire), and then alternated to the other half in a unipolar mode (Fig. 13). RF energy is delivered at all electrodes or in a selected quadrant of the MESH catheter. Once the target temperature (58°C) is reached in any thermocouple, the duty cycle is automatically varied to maintain the programmed temperature. RF energy is delivered at a maximum power of 100W for 180~300s, with target temperature of 58°C, and the maximum energy application time per PV was 900 seconds, as recommended by the manufacturer. Continuous energy delivery lasting 300 seconds was interrupted only by short preprogrammed 5-second intervals every minute to verify the circular electrogram and, hence, the ablation success. A single discrete fluoroscopically visible marker (Fig. 9D) is located at the

12-o'clock position and two other markers at the 3-o'clock position from a proximal view in order to provide visual orientation of the four quadrants of the MESH catheter.

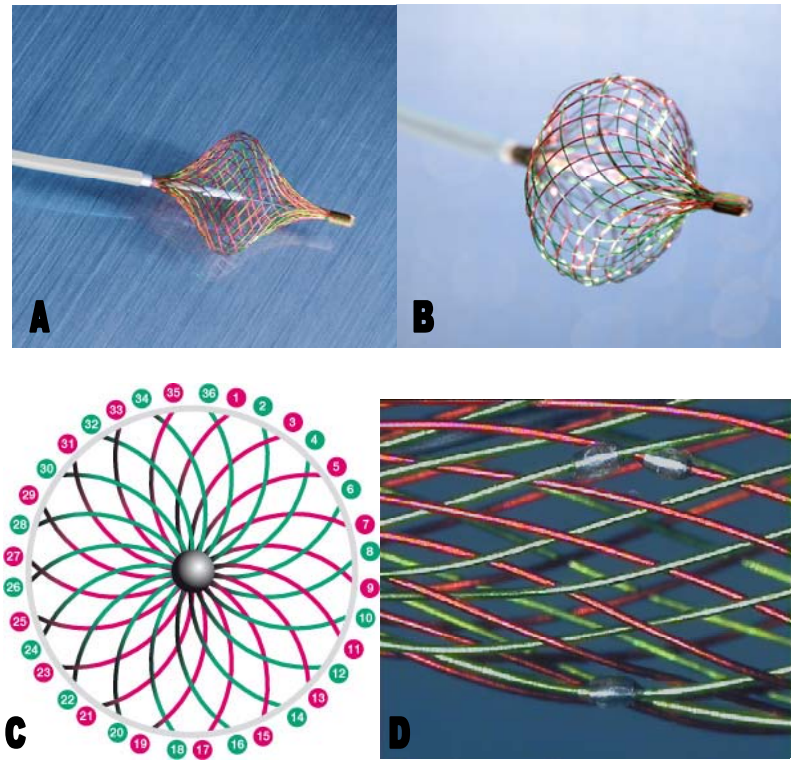


***Figure 9****.high density mesh ablator catheter ™: A novel circular mesh catheter (MESH) , designed to create curvilinear lesions at the PV-LA antrum to treat atrial fibrillation (A)8F multi-electrode-array catheter;(B) 30mm in maximum diameter;(C) 36 Bipoles on two helices of 18 wires each (maximal bipole distance 2.26mm)with covalent heparin coating; and (D) fluoro markers for orientation.*

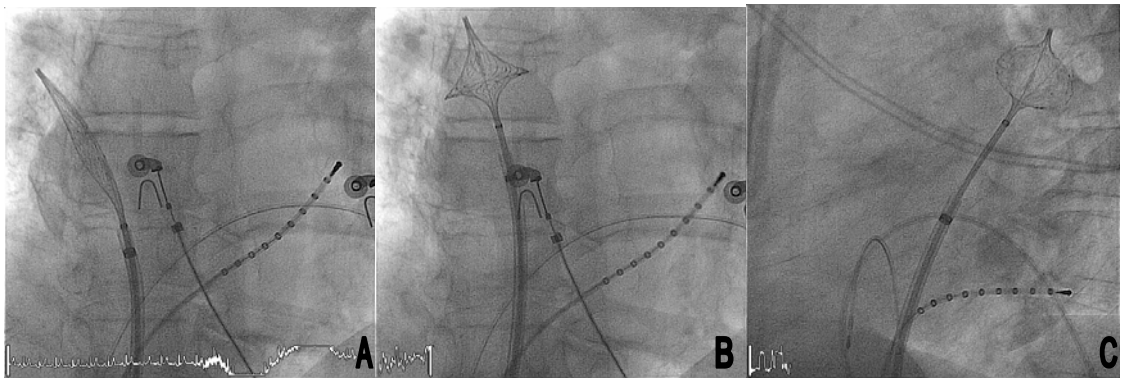


**Figure 10a**. MESH catheter *was positioned in the PV in X-ray fluoroscopy. (A)Unexpanded MESH catheter in RSPV; (B) expanded MESH catheter in RSPV; (C) expanded MESH catheter in LSPV.*

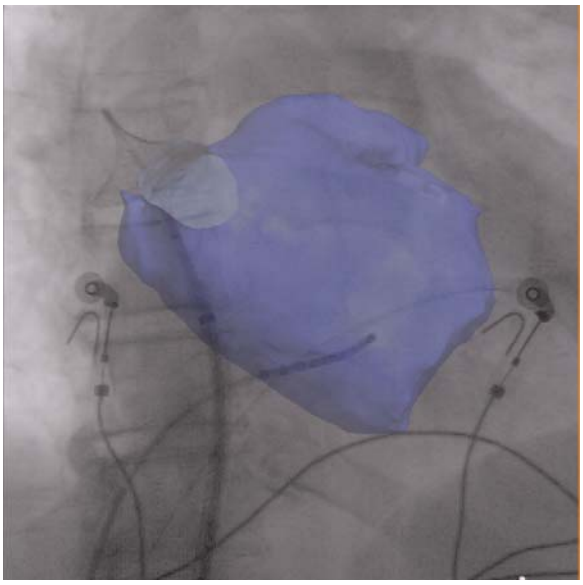

***Figure 10b**. High density mesh catheter as viewed by 3D-ATG overlapped fluoroscopy (in RSPV)*

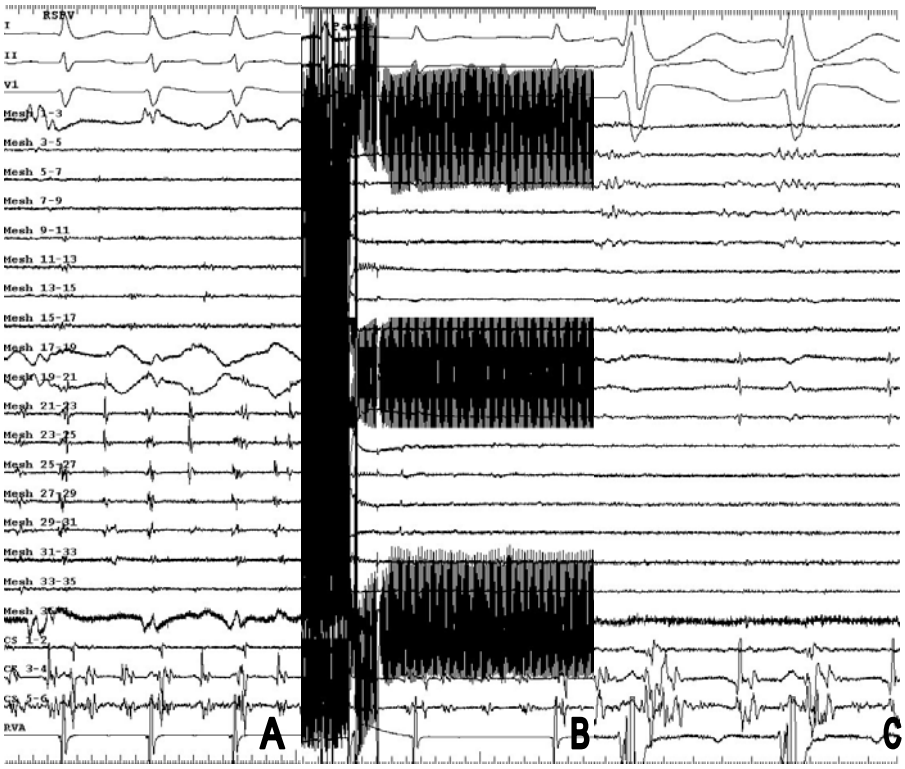


**Figure 11.** *Complete isolation of a left common PV (LCPV) in atrial fibrillation rhythm with the MESH technique. From top to bottom: surface ECG leads I, II, V1; endocardiograms in the 36-electrode MESH catheter (mesh 1-3 to mesh 35-36); endocardiograms in the coronary sinus (CS 1-2 to 5-6); signals in the right ventricular apex (RVA) (50mm/s). (A) The activity of PV potentials in the LCPV before ablation. (B) Procedure of ablation using MESH catheter. (C) Complete isolation of the LCPV after MESH ablation.*

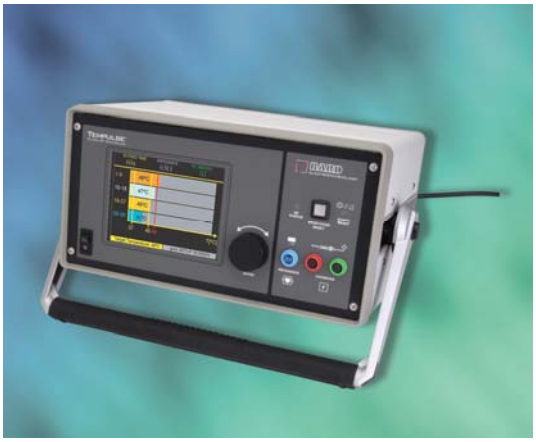

***Figure 12****.TemPulse RF controller (Bard Electrophysiology)*

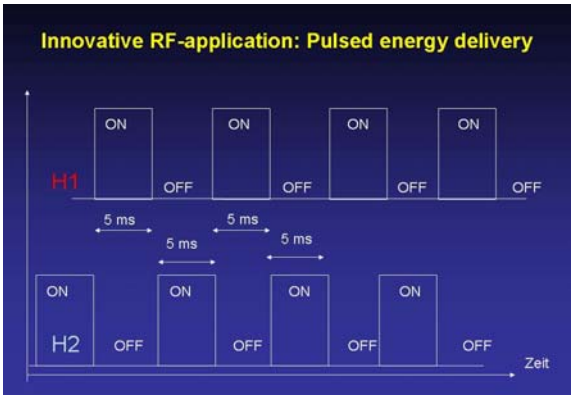


***Figure 13****. Pulsed RF energy is multiplexed into 5ms pulses and delivered through half of the electrodes (every other wire) and then alternated to the other half in a unipolar mode.*

### 3.2.5 Point-by-point RF ablation

Two transseptal punctures were performed in order to insert an ablation catheter (Navistar, Biosense Webster, 30W energy, flow 17 ml/min) and a decapolar mapping catheter (Lasso, Biosense Webster, Diamond Bar, CA, USA) into the LA (Fig. 14). Intravenous heparin was then administered to maintain a clotting time of 250 to 300 seconds. The end-point of the procedure was the electrical isolation of all PVs defined as either entrance block or elimination of PV potentials at a decapolar Lasso catheter that was positioned as closely as possible to the PV ostium (Fig. 15).

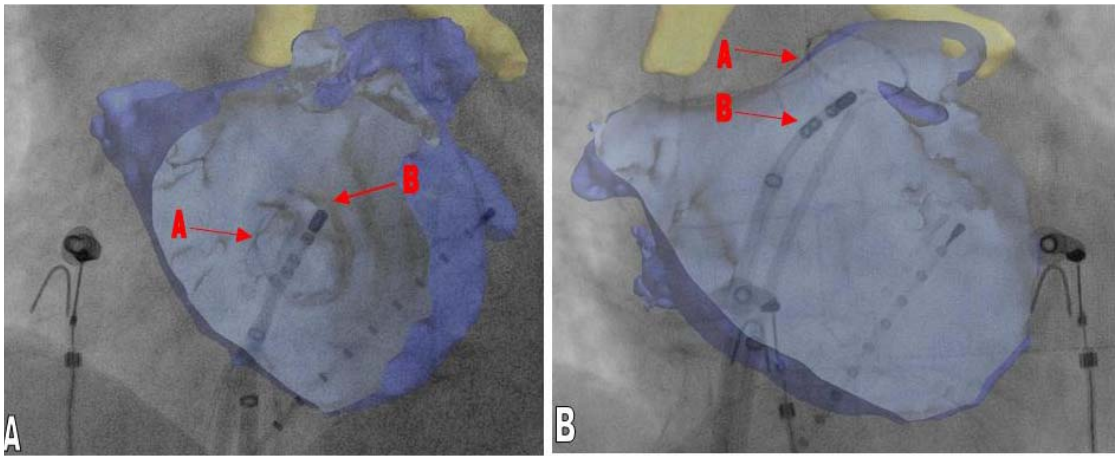


**Figure 14** *3D-ATG navigation of point-by-point RF ablation procedure. (A)RIPV, LAO 40° ;( B) LSPV, RAO 9°. A: lasso catheter; B: Navistar ablation catheter.*

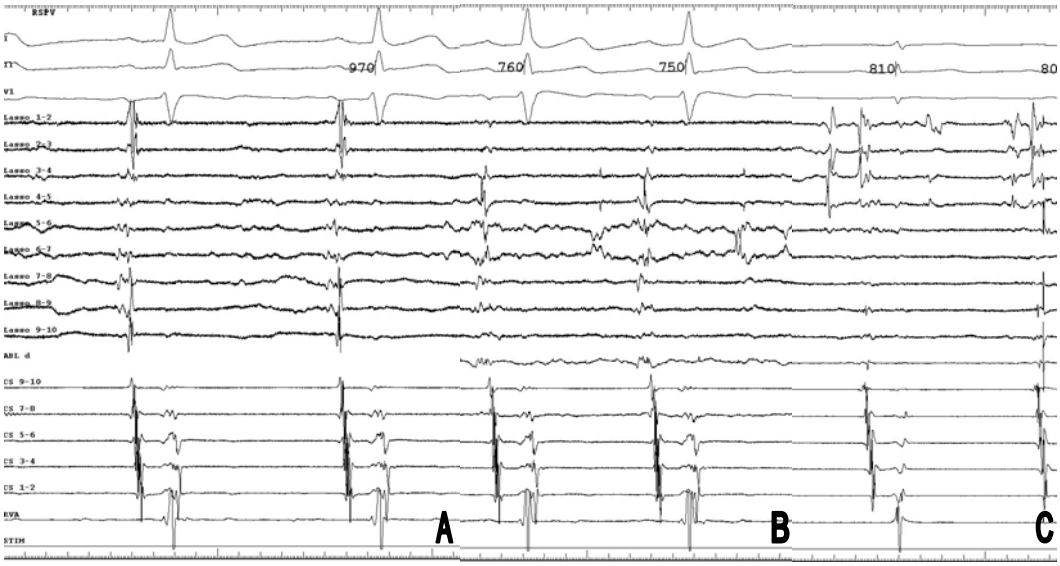


**Figure 15.** Incomplete *isolation of a right superior PV (RSPV) in sinus rhythm with the point-by-point RF technique. From top to bottom: surface ECG leads I, II, V1; endocardiograms in the Lasso catheter (Lasso 1-2 to Lasso 9-10); endocardiograms in ablation catheter (ABL-d);endocardiograms in the coronary sinus (CS 9-10 to 1-2); signals in the right ventricular apex (RVA); stimulation signal (STIM)(100mm/s). (A) The activity of PV potentials in the RSPV before ablation. (B) Ablation using RF catheter. (C) Incomplete isolation of the RSPV after RF ablation (gap at 12 o'clock position).*

### 3.3 Follow-up

On the first postprocedural day, warfarin was restarted and low-molecular heparin was administered until the international normalized ratio (INR) was >2. Warfarin was continued for

at least 3 months. Additionally, on the first postprocedural day, patients underwent a surface ECG, transthoracic echocardiography, and continuous ECG monitoring for at least 24 hours. All antiarrhythmic agents that were discontinued prior to the procedure were recommenced, with a view to stopping all antiarrhythmic agents after 3 months if patients remained free from AF. A 3-month blanking period was applied so that any AF recurrence during this period was not considered as treatment failure. Follow-up visits in the outpatient clinic were planned at 1, 3, 6, and subsequently 6 monthly intervals after ablation. Patients reported having or not having symptoms (Scores 1-5: 1= no improvement of symptoms; 2= mild improvement; 3= moderate improvement; 4= significant improvement; 5= no symptoms at all) at each visit. A 24-hour Holter ECG and a cardiac magnetic resonance imaging examination were performed at each follow-up visit.

Endpoints: recurrence of AF was defined as the presence of at least one recording of AF after ablation, regardless of its origin (12-lead ECG, transtelephonic rhythm strip, 24h Holter recording, or unsolicited tracing).

### 3.4 Statistical analysis

Continuous variables were expressed as the mean value ± SD (standard deviation) and compared with the one-way analysis of variance or *t*-test. A Pearson chi-square test or Fisher's exact test was used for categorical variables. Nonparametric tests were used when appropriate. Actuarial event-free rates from AF were calculated according to the Kaplan-Meier method and were compared by use of the log-rank test. Multivariable Cox models were employed to assess the independent predictors of arrhythmia recurrence after PV isolation. *P* value <0.05 was considered statistically significant. Statistical analysis was performed using SPSS, version 17.0 (SPSS Inc.).

## 4. Results

### 4.1 Patients' characteristics

A total of 176 patients aged 61±11 years were included. Fifty-two patients were randomized

to the cryoballoon group, 46 patients to PVAC ablation groups, and 52 patients to the open-irrigation RF ablation catheter group, but only 26 patients were randomized to the MESH group due to the shortage of MESH catheters in the later period of the study. All patients had symptomatic AF resistant to 2±1 drugs with a median of one previous external cardioversion. The time since the initial diagnosis of AF to the ablation procedure was 63±75 months (1~468months). Of 176 patients, 118 (67.0%) had paroxysmal AF and 58 patients (33%) had persistent AF. Details for the clinical demographic data of the patients are shown in Table 1.

Table1. Baseline characteristics of patients who underwent ablation using different catheters

| *Patient* | *Cryoballoon (n=52)* | *PVAC (n=46)* | *MESH (n=26)* | *RF (n=52)* | ***Total (n=176)*** | ***P* value** |
|---|---|---|---|---|---|---|
| Male, n (%) | 39 (75) | 32 (70) | 20 (77) | 22 (42) | 113(64) | >0.05 |
| Age (y) | 60±11 | 62±11 | 61±9 | 61±11 | 61±11 | >0.05 |
| History of AF (m.) | 57±79 | 58±60 | 63±87 | 73±80 | 63±75 | >0.05 |
| Paroxysmal AF (%) | 41(78.8) | 32(70.0) | 13(50.0) | 32(61.5) | 118(67.0) | >0.05 |
| Persistent AF | 11 | 14 | 13 | 20 | 58 | >0.05 |
| LVd (mm) | 51.7±5.0 | 51.7±6-3 | 51.5±7.0 | 48.6±5.2 | 50.7±5.9 | >0.05 |
| LVs (mm) | 34.8±7.2 | 34.2±7.1 | 35.2±7.5 | 31.8±6.4 | 33.8±7.1 | >0.05 |
| LA (mm) | 45.1±5.1 | 45.6±7.5 | 46.5±7.1 | 44.0±7.4 | 45.1±6.8 | >0.05 |
| LVEF (%) | 61.4±10.5 | 61.2±11.2 | 61.6±11.9 | 63.4±10.4 | 62.0±10.8 | >0.05 |
| Hypertension (%) | 33 (63.5) | 39 (84.8) | 19 (73.1) | 34(65.4) | 125 (71.0) | >0.05 |
| Diabetes mellitus (%) | 5 (9.6) | 3 (6.5) | 4 (15.4) | 8 (15.4) | 20 (11.4) | >0.05 |
| CAD requiring CABG or PCI (%) | 10 (19.2) | 10 (21.7) | 11 (2.3) | 10 (19.2) | 41 (23.3) | >0.05 |
| SHD (%) | 5 (9.6) | 0 | 0 | 1 (1.9) | 6 (3.4) | >0.05 |
| Cardiomyopathy (%) | 2 (3.8) | 2 (4.3) | 2 (7.7) | 2 (3.8) | 8 (4.5) | >0.05 |
| VHD (%) | 3 (5.8) | 1 (2.2) | 2 (7.7) | 2 (3.8) | 8 (4.5) | >0.05 |

y= year; m= months; mm=millimeter; LVd=left ventricular end-diastolic diameter; LVs=left ventricular end-systolic diameter; LA= left atrium; LVEF=left ventricular ejection fraction; CAD=coronary artery disease; CABG= coronary artery bypass graft; PCI= percutaneous coronary intervention; SHD=structural heart disease; VHD=valvular heart disease.

### 4.2 Immediate procedural data

In the 176 study patients, the mean procedure duration was 155.2±43.8 minutes, with a fluoroscopy time of 35.5±14.6 minutes and a mean ablation time of 32.6±14.7 minutes. The mean procedure time was shortest in the PVAC group and longest in the RF group. Pairwise comparison between each two groups was made; there was no significant difference only

between the PVAC group and MESH group (*P*=1.00) (Fig. 16). However, the fluorotime was shortest in the MESH group and longest in the RF group. No significant difference were found between the PVAC group and the MESH group (P=0.14) or between the cryoballoon group and the PVAC group (*P*=0.12) (Fig. 17) by pairwise comparison. The PVAC group had the shortest ablation time and the cryoballoon group had the longest ablation time. There was a significant difference in total ablation time in the cryoballoon group compared with the PVAC group, the PVAC group compared with the MESH group, and the PVAC group compared with the RF group (Fig. 18).

Details of the immediate procedural data were presented in Table 2. The immediate procedural data for the 118 paroxysmal AF patients are shown in Table 3. Mean procedure time was 152.9±43.6 minutes; mean fluorotime was 35.0±14.5 minutes; and mean ablation time was 32.1±14.8 minutes.

Acute procedural success was achieved in 73.3% (129/176) of patients. Complete PV isolation was achieved in 71.2% (37/52) of patients in the cryoballoon group, 76.1 % (35/46) of patients in the PVAC group, 65.4% of patients in the MESH group, and 76.9% (40/52) of patients in the RF group (chi-square test: *P*>0.05). For all the patients, 644/704 (91.5%) targeted PVs were successfully isolated; 168/176 (95.5%) targeted LSPVs, 163/176 (92.6%) targeted LIPVs, 162/176 (92.0%) targeted RSPVs, and 149/176 (91.5%) targeted RIPVs were successfully isolated. The isolation of PVs in the four ablation technique groups is compared in Table 4. There was no significant difference in the success of isolation for every PV among the four groups. In the MESH group, there was no ablation in 5 RIPVs because the pulmonary veins were too small to be entered.

In the 184 PVs that were isolated with simplified cryoballoon technique, PV isolation was monitored in real time during the cryoablation in 172 PVs (93.5%) and the isolation was checked immediately after ablation in 16 PVs (6.5%). It could not be monitored in real time during PVAC ablation or MESH ablation because of the electrical interference during ablation.

In addition, we performed a linear right atrial isthmus ablation in 3 patients in the cryoballoon group and 2 patients in the RF group who also presented with typical atrial flutter. Bidirectional block was achieved in all patients.

Table 2. Comparison in patients undergoing different catheter ablations

| | Cryoballoon | PVAC | MESH | RF | total | *P* value |
|---|---|---|---|---|---|---|
| Mean procedural time (min.) | 157.8±42.6 | 125.2±28.7 | 134.5±34.4 | 189.8±34.9 | 155.2±43.8 | <0.001 |
| Fluorotime(min.) | 36.6±14.2 | 30.5±11.3 | 23.4±9.3 | 45.0±13.5 | 35.5±14.6 | <0.001 |
| Mean ablation time (min.) | 38.9±13.8 | 21.6±7.7 | 35.4±15.8 | 36.1±14.6 | 32.6±14.7 | <0.001 |
| Ablation time of LSPV (min.) | 19.4±9.2 | 12.9±9.5 | 14.1±11.6 | 25.7±20.5 | 18.7±14.4 | <0.001 |
| Ablation time of LIPV (min.) | 17.6±11.9 | 10.6±6.6 | 12.2±8.4 | 12.8±10.4 | 13.7±10.1 | 0.008 |
| Ablation time of RSPV (min.) | 14.7±10.2 | 11.5±6.5 | 15.9±9.3 | 19.3±17.1 | 15.4±12.2 | 0.024 |
| Ablation time of RIPV (min.) | 8.4±7.7 | 11.3±8.1 | 8.4±8.1 | 16.2±13.7 | 11.5±10.4 | 0.001 |
| Ablation time of LCPV/RMPV (min.) | 16.0±5.7 | 25.3±12.8 | 27.5±3.5 | 33.6±14.2 | 27.4±12.3 | 0.417 |
| DAP (mGy*cm$^2$) | 218868.5±156338.5 | 123556.0±97722.5 | 151356.5±100437.3 | 149441.4±84530.0 | 163471.3±120470.2 | 0.001 |

DAP= Radiation dosis as dose area product (mGy cm$^2$); LSPV=left superior pulmonary vein; LIPV= left inferior pulmonary vein; RSPV=right superior pulmonary vein; RIPV= right inferior pulmonary vein; LCPV= left common pulmonary vein; RMPV= right middle pulmonary vein.

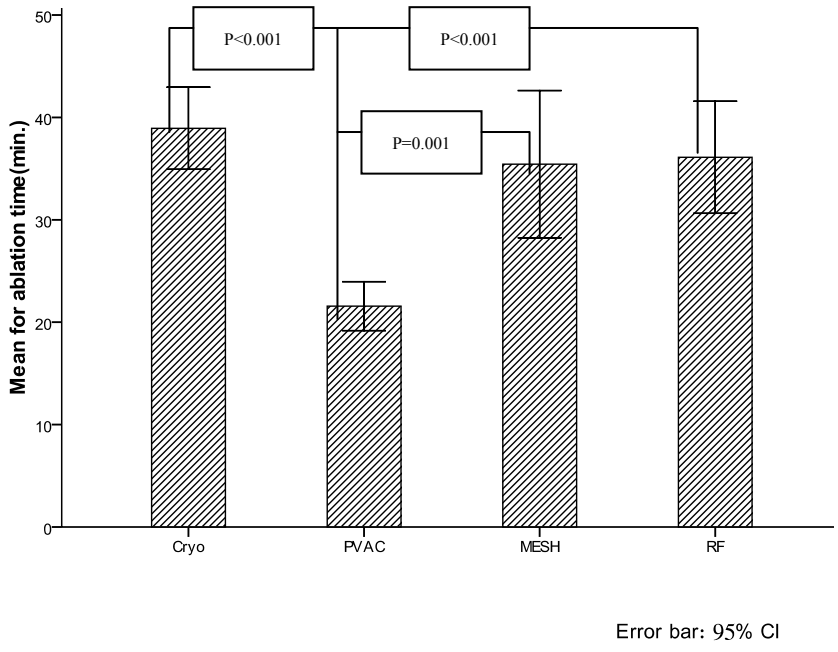


Figure 18. *Bar graph for the ablation time of different groups*

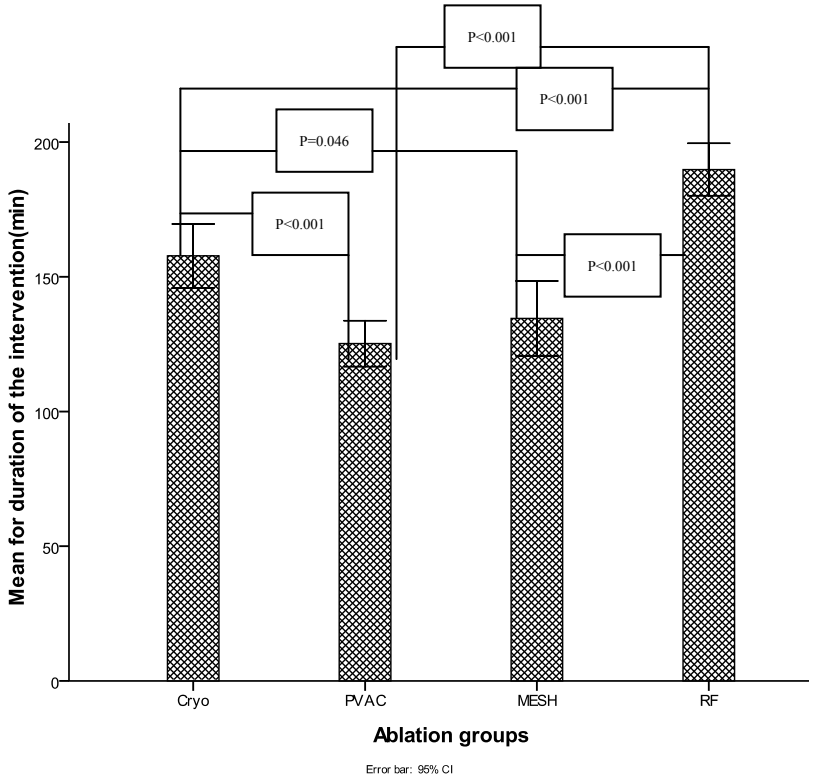


Figure 16. *Bar graph for the total procedure time of different groups*

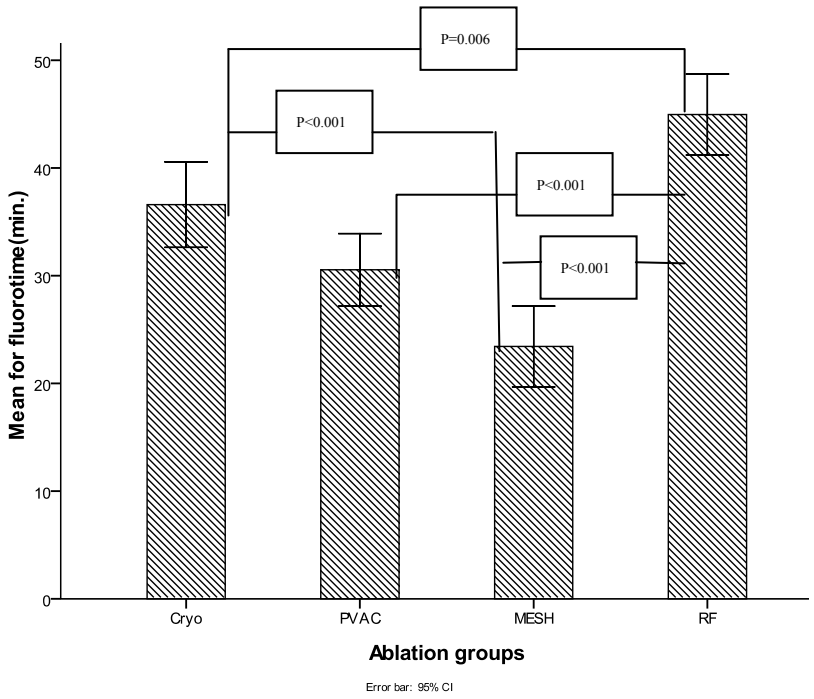


Figure 17. *Bar graph for the fluorotime of different groups*

Table 3. Comparison in patients with paroxysmal AF undergoing different catheter ablations

| | Cryoballoon | PVAC | MESH | RF | Total | P value |
|---|---|---|---|---|---|---|
| Mean procedural time (min.) | 158.2±44.7 | 123.7±25.7 | 131.5±39.8 | 183.9±35.2 | 152.9±43.6 | P<0.001 |
| Fluorotime(min.) | 37.2±15.4 | 29.4±9.8 | 22.7±10.9 | 42.6±13.4 | 35.0±14.5 | P<0.001 |
| Mean ablation time (min.) | 38.1±14.0 | 20.5±6.0 | 34.7±17.6 | 36.5±14.7 | 32.1±14.8 | P<0.001 |
| Ablation time of LSPV (min.) | 19.7±9.4 | 11.5±7.5 | 15.2±13.2 | 28.6±21.2 | 19.0±14.5 | P<0.001 |
| Ablation time of LIPV (min.) | 16.7±11.9 | 10.2±6.1 | 13.6±9.7 | 10.6±8.2in | 13.1±9.8 | P=0.025 |
| Ablation time of RSPV (min.) | 14.8±11.2 | 11.5±5.8 | 15.8±10.9 | 23.0±20.3 | 16.1±13.8 | P=0.012 |
| Ablation time of RIPV (min.) | 8.0±7.9 | 11.4±7.2 | 6.5±5.6 | 14.7±10.9 | 10.4±8.8 | P=0.007 |
| Ablation time of LCPV/RMPV (min.) | 16.0±5.7 | 28.0±14.2 | 31.7±16.1 | 26.4±13.4 | 26.4±13.4 | P=0.497 |
| DAP (mGy*cm$^2$) | 221823.8±167093.6 | 118288.9±94540.4 | 128958.0±63225.5 | 140742.0±86235.8 | 161527.3±127731.5 | P=0.002 |

DAP= Radiation dosis as dose area product (mGy cm$^2$); LSPV=left superior pulmonary vein; LIPV= left inferior pulmonary vein; RSPV=right superior pulmonary vein; RIPV= right inferior pulmonary vein; LCPV= left common pulmonary vein; RMPV= right middle pulmonary vein.

Table 4. Isolation of the PVs using different catheters

| | Cryoablation | | PVAC ablation | | MESH | | RF | | total | |
|---|---|---|---|---|---|---|---|---|---|---|
| | isolated(%) | unisolated | isolated(%) | unisolated | isolated(%) | unisolated | isolated(%) | unisolated | isolated(%) | unisolated |
| LSPVs* | 50(96.2) | 2 | 43(93.5) | 3 | 25(96.2) | 1 | 50(96.2) | 2 | 168(95.5) | 8 |
| LIPVs* | 47(90.4) | 5 | 45(97.8) | 1 | 22(84.6) | 4 | 49(94.2) | 3 | 163(92.6) | 13 |
| RSPVs* | 48(92.3) | 4 | 44(95.7) | 2 | 25(96.2) | 1 | 45 (86.5) | 7 | 162(92.0) | 14 |
| RIPVs* | 39(75.0) | 13 | 43(93.5) | 3 | 20(76.9) | 6 | 47(90.4) | 5 | 149(84.7) | 27 |
| Total* | 184(88.5) | 24 | 175(95.1) | 9 | 94(90.4) | 12 | 191(91.8) | 17 | 644(91.5) | 60 |

* Fisher's exact test: $P>0.05$.

### 4.3 Complications

In the cryoballoon group, phrenic nerve palsy (PNP) was detected during RSPV isolation in one case (1/52, 1.9%), which was resolved 3 months post ablation as documented with fluoroscopic evaluation of the diaphragmatic movement. Phrenic nerve palsy was also observed in another patient before the procedure of PV isolation using cryoablation, which lasted during the following-up checks and was probably due to disease of cervical vertebrae which she had

had for several years. Air embolism was observed in one patient (1/46, 2.2%) undergoing PVAC ablation after transseptal puncture with ST segment elevated on surface ECG and persisted for 20 minutes, then recovered after adrenaline was given intravenously. In 2 patients undergoing PVAC ablation (2/46, 4.3%) and 1 patient (1/26, 3.8%) undergoing MESH ablation, mild pericardial effusion was detected on the first postprocedural day and absorbed within 1 week. Tamponade was observed in one patient undergoing MESH ablation (1/26, 3.8%) which needed pericardial puncture. No incidence of PV stenosis was observed during the whole follow-up period with MRI in all the patients. The complication rates were 1.9% (1/52) of cryoballoon, 6.5% (3/46) of PVAC, and 7.7% (2/26) of MESH with no significant differences. The complication rate of the whole study cohort was 4.8%.

### 4.4 Follow-up

The mean follow-up was 11±8 months (3-39 months) until April 30th 2011 for all the patients recruited; mean follow-up in different groups is shown in Table 5 ($P$>0.05). During follow-up, patients assessed improvement in their symptoms captured in a self-scoring system which ranged from 1 to 5: 1=no improvement of symptoms, 2= mild improvement, 3=moderate improvement, 4= significant improvement, and 5=no symptoms at all. The mean score was 4±1. A total of 124/176 (69.3%) patients reported significantly improved symptoms or were entirely asymptomatic. Thirty-one (59.6%) of 52 patients undergoing cryoablation, 31 (67.4%) of 46 patients undergoing PVAC ablation, 13/26 (50%) patients in the MESH group, and 33/52 (35.3%) patients in the RF group were reported to be free from atrial fibrillation at the end of follow-up. The statistical event-free rates from any AF for four groups were calculated and are shown in Fig. 19; no significant difference was found among them ($P$=0.25). Kaplan-Meier curves for cryoballoon versus RF, PVAC vs. RF, and MESH vs. RF are shown in Fig. 20- 22. All the three groups had lower rates of AF recurrence compared with the RF groups without statistically significant difference. The statistical event-free rates from any AF for paroxysmal AF patients who underwent four catheter ablation procedures are shown in Fig. 23, and there was also no significant difference among the four groups. Seventy-three of 118 (61.9%) paroxysmal AF patients and 37/58 (35.1%) persistent AF patients were reported to be free from

atrial fibrillation at the end of follow-up with statistically significant difference ($P$<0.001). The mean follow-up was 12±9 months for the paroxysmal AF patients, and 9±7 months for the persistent AF patients (Fig. 24). In multivariable analysis, the type of AF was the only independent predictor of early arrhythmia recurrence after ablation (RR 1.96, P=0.001).

Table 5. Follow-up parameters for different groups

| | Cryoballoon | PVAC | MESH | RF | Total |
|---|---|---|---|---|---|
| Follow-up time (months)* | 12±8 | 8±5 | 11±9 | 12±9 | 11±8 |
| Freedom from AF (%) $^{\Delta}$ | 31 (59.6) | 31 (67.4) | 13 (50.0) | 18 (35.3) | 93 (53.1) |

* $P$=0.063; $\Delta$ $P$=0.25

Table 6. Recurrence of AF after ablation during follow-up

| | 3 months | 6 months | 12 months | 24 months | Follow-up time (month) |
|---|---|---|---|---|---|
| Paroxysmal AF$^{\Delta}$ | 14.4$^{*}$ (17/118) | 21.2 (25/118) | 32.2 (38/118) | 37.3(44/118) | 12±9 |
| Persistent AF$^{\Delta}$ | 33.3 (19/57) | 47.4 (27/57) | 57.9 (33/57) | 64.9 (37/57) | 9±6 |

*: the ratio of recurrence of AF; $\Delta$: $P$=0.003.

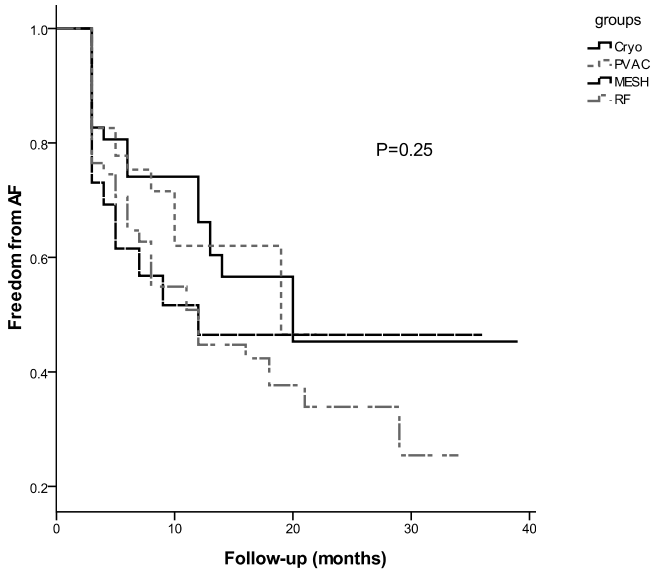


**Figure 19** *Kaplan-Meier graphs showing the atrial fibrillation-free survival in the cryoballoon group, PVAC group, MESH group and RF group. Log rank test: P=0.25.*

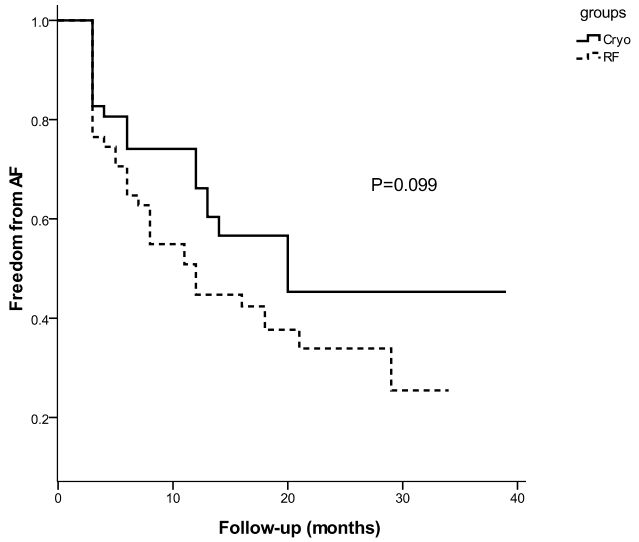


**Figure 20** *Kaplan-Meier graphs showing the atrial fibrillation-free survival in the cryoballoon group and RF group. Log rank test: P=0.099.*

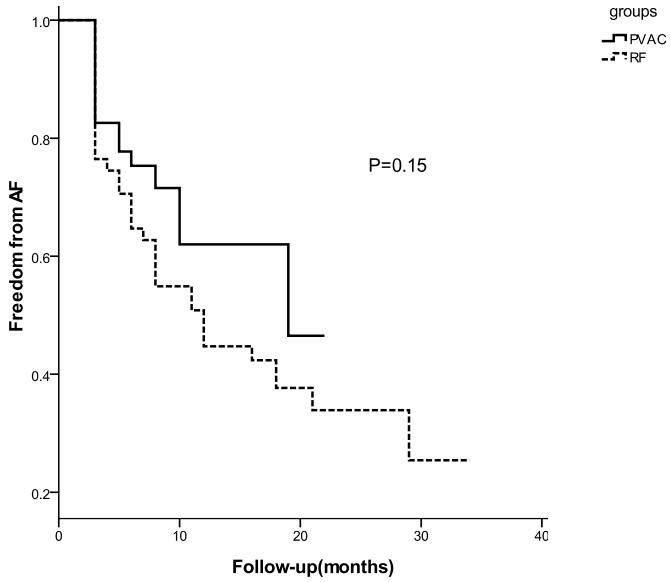


**Figure 21** *Kaplan-Meier graphs showing the atrial fibrillation-free survival in the PVAC group and RF group. Log rank test: P=0.15.*

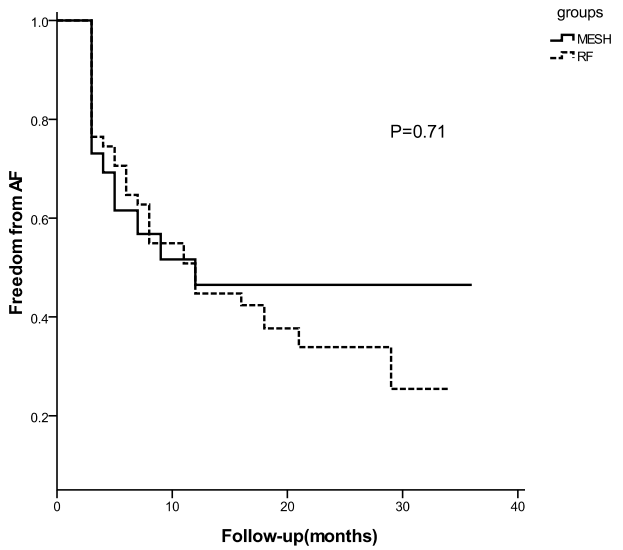


**Figure 22.** *Kaplan-Meier graphs showing the atrial fibrillation-free survival in the MESH group and RF group. Log rank test: P=0.71.*

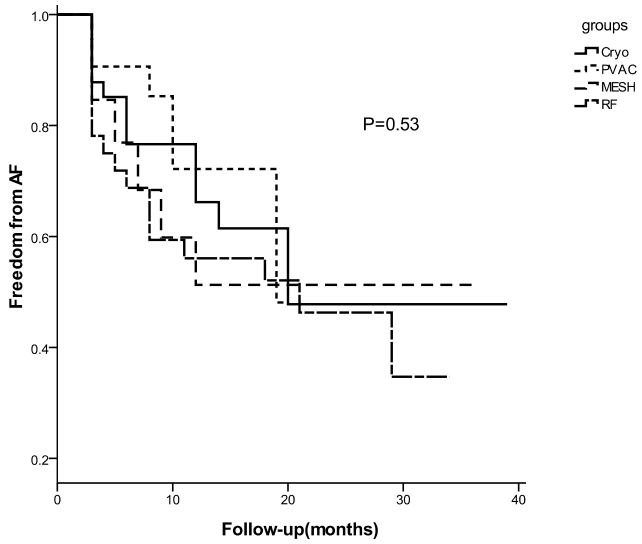


**Figure 23** *Kaplan-Meier graphs showing the atrial fibrillation-free survival in the paroxysmal AF patients using Cryoballoon, PVAC, MESH, or RF technique. Log rank test: P=0.53.*

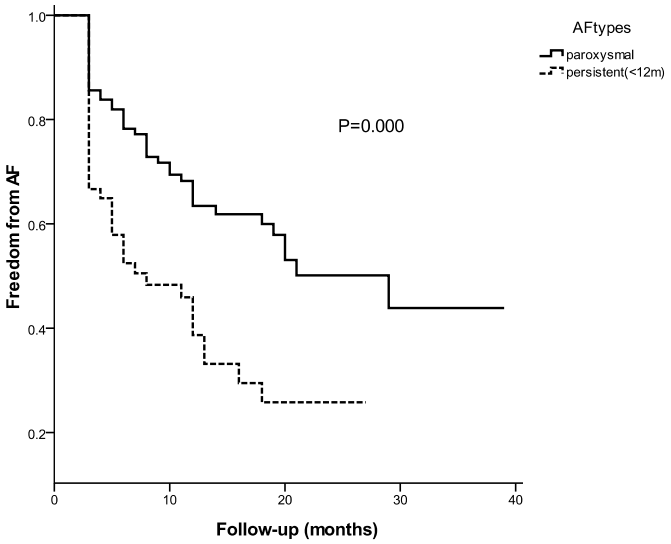


**Figure 24** *Kaplan-Meier graphs showing the atrial fibrillation-free survival in the paroxysmal AF patients and persistent AF patients. Log rank test: P=0.000.*

## 5. Discussion

The high prevalence of AF and the limitations of available antiarrhythmic drugs have made catheter ablation an important therapy in patients with symptomatic AF. PV isolation is currently the most well-accepted ablation strategy for the treatment of AF because of the demonstration of a pathophysiological role of PV myocardium and a simple and unambiguous endpoint [1]. Although data of the outcomes for catheter ablation of AF derived from large prospective randomized multicenter trials are needed, recent randomized clinical trials comparing the outcomes of catheter ablation and antiarrhythmic drugs have shown that the AF freedom rate was 66-89% without any antiarrhythmic drugs in the ablation group, as compared with 17-43% in the antiarrhythmic medication group [3]. Moreover, catheter ablation was also associated with better symptomatic relief and exercise tolerance as compared with arrhythmic medication [3]. In our study, 69.3% patients reported significant symptom improvement or were entirely asymptomatic no matter the AF freedom rate. Catheter ablation successfully treats paroxysmal AF in 41-94% of patients, and in 20-61% of persistent AF cases freedom from AF could be achieved by pulmonary vein isolation alone[60]. We achieved catheter ablation success in 61.9% of paroxysmal AF patients and 35.1% of persistent AF patients.

Up to now, most EP laboratories still use a circular mapping catheter and a standard 3.5-mm irrigated tip ablation catheter, which is often a time-consuming point-to-point ablation approach and the application of RF energy has been associated with complications such as PV stenosis, stroke, atrio-esophageal fistula, left atrial flutter, and pericardial effusion. Thus, new energy sources as well as new catheters are under development and investigation in order to simplify the procedure and reduce complications. Theses include cryoballoon technique, PVAC system, MESH catheter, and others. However, reports about direct comparison regarding efficacy and safety among these novel ablation techniques are absent. This is the first time we have compared the efficacy and safety of these four techniques. Also in this study, we introduced a novel simplified cryoballoon technique, which was first reported by Tang M et al. of our center in 2010 [35].

### 5.1 Efficacy

In our study, all the three novel techniques had shorter procedural time, shorter fluorotime, and shorter ablation time as compared with RF ablation technique (Table 2, Fig. 14-16). Among these 3 novel ablation techniques, PVAC had the shortest procedural time and ablation time and MESH had the shortest fluorotime. Hofmann R et al. reported a comparison between the MESH ablator and traditional cryoballoon catheters and showed similar procedural and fluoroscopy times in the two groups [61]. Bulava A. et al. compared traditional PVAC with RF catheter guided by CARTO in paroxysmal AF patients and found that the use of PVAC ablation significantly reduced total procedural and fluoroscopic times while achieving the same efficacy [62] as RF ablation.

Complete PV isolation was achieved in 73.3% (129/176) of patients, and 91.5% (644/704) of target veins were successfully isolated. Patients in the RF group achieved the highest ratio of complete PV isolation (76.9%), and patients in the PVAC group achieved the highest ratio of target vein isolation (95.1%), but the difference did not reach statistical significance. All the techniques achieved a relatively lower ratio of isolation in RIPV compared with the other three PVs; a possible explanation may be that the RIPVs were relative small and not easy to enter. We had a similar acute success as reported [26] [40-44] [62] [63].

Concerning the cryoballoon technique, a meta-analysis for 23 conventional cryoballoon studies showed that the average procedural time was 206.3±72.2 minutes (range 108-371 minutes), with fluoroscopy time of 46.0±13.3 minutes (range 20.1-84.5 minutes), which was longer than our results for the simplified cryoballoon technique (157.8±42.6min and 36.6±14.2min, respectively) [26]. The most likely reason was the relative simplification of the cryoballoon technique (just one transseptal puncture). Another reason may be the utilization of 3D-ATG instead of 3D mapping system in the procedure of PV isolation, which reduced the procedure time compared with 3D mapping system as described in Part II, but further study is needed to validate this. In our cryoballoon procedure, isolation was observed in real time during ablation in 93.5% of the veins. The mapping wire had to be positioned deep inside the target PV during ablation in 6.5% of target veins to facilitate complete balloon occlusion of the vein. It was subsequently withdrawn immediately post ablation to record residual PV potentials. This is

a relatively easy-to-perform technique and does not appreciably contribute to case times. Andrade et al. reported that ablation with the conventional cryoballoon catheter alone (i.e., excluding concomitant focal ablation) resulted in PVI in 92.64% (95% CI [confidence interval] 91.76%-93.45%) of targeted veins and complete PVI in 77.81% of patients (95% CI 74.99%-80.45%) in a review of 23 studies for conventional cryoballoon technique [27], while we achieved PVI in 88.5% of targeted veins and complete PVI in 71.2% of patients in the cryoballoon group. However, following our previously defined approach, no additional conventional ablation catheter was used if a PV could not be successfully isolated. This helped considerably to keep the procedure time short. We also included both paroxysmal AF and persistent AF subjects while most of other studies included only paroxysmal AF subjects. Therefore a direct comparison between these data is not accurate.

According to the long-term outcomes, at the end of follow-up (mean 11±8 months, range 3-39 months), 59.6% of patients in the cryoballoon group, 67.4% of patients in the PVAC group, 50.0% of patients in the MESH group, and only 35.3% of patients in the RF group were free of recurrent AF without antiarrhythmic drugs, but the difference did not reach statistical significance. Also, no significant difference of freedom from atrial fibrillation recurrence among the four groups was found in paroxysmal AF patients. Comparing the clinical success of three novel ablation techniques with conventional RF ablation showed that all of them had lower recurrence rates of AF than the RF ablation technique, but without statistical difference. There was a significant difference between the paroxysmal AF patients and persistent AF patients ($P$<0.001), and in multivariable analysis, only the type of AF (RR 1.96, P=0.001) was an independent predictor of early arrhythmia recurrence after ablation, which was validated by Weerasooriya et al [64].

The acute success rate and clinical success for the MESH group was relatively lower compared to the cryoballoon or PVAC group and but was similar to that given in previous reports [45-47] [65]. An important factor for the poor outcome of MESH technique may be related to unfavorable angulations of the PV ostia relative to the MESH catheter. This leads, in some situations, to a mismatch between the shaft of the MESH catheter and the axis of the vein and may results in suboptimal contact with all the available electrodes. Another reason for the poor outcome might be the inadequacy of the depth of penetration using MESH technique; the

duration of the energy delivery was 300s. The mapping and energy-delivering electrodes of the MESH are positioned 2mm distally to the equator to enable optimal tissue contact when the device is pushed toward the PV ostium for ablation. Thus, the mapping electrodes are in less direct contact with the PV tissue when mapping the electrical ostium of the PVs. This could lead to inaccurate mapping before and after the ablation, resulting in false information according to the presence or absence of PV potentials [45]. The main goal for long-standing PVI is ablation of the PV potentials as well as the deep, almost transmural lesion. The energy delivery by the thin mesh electrodes probably does not lead to transmural penetration and consequently does not produce sufficient isolation of the PV-LA junction as required in AF. Another reason might be that the essential part of the MESH is in less direct contact with the PV tissue, leading to inaccurate mapping before and after the ablation and resulting in false information according to the presence or absence of PV potentials [45]. This hypothesis is strengthened by the results recently reported by Pappalardo et al, who found lower rates of PV isolation with the MESH alone. When acute ablation results were confirmed with conventional spiral catheter confirmed PV isolation after ablation with the MESH alone the 1-year follow-up success rate was much higher (80%) than the rate observed in our series [66].

### 5.2 Safety

Complications of catheter ablation procedures are often evident and can be directly linked to the intervention. In recent systematic literature reviews and meta-analyses on antiarrhythmic medications for AF, a major complication of AF ablation occurred in 4.9% of patients [66].

In our study, no serious complications were noted in the RF group. Phrenic nerve palsy (PNP) was detected in one of 52 patients underwent cryoablation (1.9%). Two cases of air embolism were noted in the PVAC group, and 2 patients in this group had mild pericardial effusion. Two patients in the MESH group also had pericardial effusion, of which one was mild pericardial effusion and one was pericardial tamponade. No incidence of PV stenosis was noted during the follow-up in any of the patients. The complication rate was relatively higher in the MESH group without significant differences, which may be due to the relatively small sample of patients in the MESH group. Kojodjojo et al[67] aggregated complication rates from

cryoballoon procedures on 611 patients reported in 3 large series of patients at 5 different European hospitals and found that vascular access complications such as groin hematomas occurred in 1.6% of patients; 1.8% developed pericardial effusions requiring drainage, but surgical repair was not necessary. These rates are comparable with those for radio-frequency ablation. There were no strokes, and atrioesophageal fistulation has not been reported with cryoablation. Meta-analysis reported that the most common complication was PNP, with an overall incidence of 6.38% (86/1,349 procedures). The incidence of PNP persisting after the ablation procedure was 4.73% (67/1,349). Delayed recovery was the predominant outcome; with only 0.37% (5/1,349) experiencing PNP that persisted beyond 1 year [26]. For the simplified cryoballoon technique, we achieved relatively lower PNP which should be validated by further study with a larger sample.

### 5.3 Limitations

Simplified cryoballoon technique, PVAC technique, and MESH technique all have the same advantage that they can be performed using a single transseptal puncture which makes the procedure less complex. However, each of them has limitations. The common limitation was the suitability of the pulmonary venous anatomy. The biggest drawback is the single size of the catheter available on the market at present. For the cryoballoon technique, we utilized a single size of balloon (28mm in diameter) and the diameter (15mm) of the mapping catheter is also small; patients with large common ostia were excluded. The balloon could not achieve complete contact when the vein was smaller or bigger, which made intubation of large veins more difficult and increased the risk of PNP. For the PVAC technique, bigger veins (>25mm in diameter) must actually be isolated in an almost point-by-point manner even when using the PVAC - rotating the catheter and maneuvering it against the antra of the vein around its entire circumference [59]. For MESH, suitable anatomic conditions were given, defined by the presence of four clearly separated PVs with a maximal ostial diameter of between 15 and 25mm and a LA diameter of <50mm. The available MESH array had a maximum diameter of 30mm, leading fluoroscopically to complete contact [44].

The most important complication of cryoballoon ablation is PNP even with close monitoring

of phrenic movement [65], which frequently occurs by ballooning deep in the PV, especially in the right superior PV with a 23mm balloon [31]. Most instances of PNP are fully regressive during follow-up of less than 1 year. In contrast, however, it has been demonstrated that esophageal injury or atrial-esophageal fistula develops rarely after cryoballoon ablation [26].

For PVAC, another limitation is that the catheter is almost unadjustable in the diameter due to the fixed circumference, which made intubation of small veins for controlling isolation challenging. Also, it is impossible to observe PV signals while ablating, which makes the interpretation of signals more difficult and probably represents the main limitation of the system as compared with the conventional approach and simplified cryoballoon approach. Furthermore, the cross-talk between the proximal electrode and distal electrode on RF delivery due to the design of the catheter impacted the RF application effect.

For the MESH catheter, another limitation is also the impossibility of observing PV signals while ablating.

# Part II Comparison between the conventional electroanatomical system and image-integration of intra-procedural rotational angiography-based 3D reconstructions of left atrium and pulmonary veins during catheter ablation for atrial fibrillation

## 3. Methods

### 3.1 Patient selection

Patients with symptomatic, medically refractory AF registered for ablation between January 2007 and December 2008 at the German Heart Institute Berlin were recruited. The inclusion criteria and exclusion criteria were described in Part I. All patients were randomly divided into two groups: (1) point-by-point RF ablation guided by CARTO; (2) point-by-point RF ablation guided by 3D-ATG.

Transesophageal echocardiography was performed prior to the procedure to exclude left atrial thrombus. All patients signed informed consent, and the study was performed in accordance with the Institutional Research guidelines of the German Heart Institute Berlin.

### 3.2 Procedure

#### 3.2.1 Conventional electroanatomical system (CARTO)

Electroanatomical procedures were performed using an electromagnetic localization system (CARTO, Biosense-Webster, Inc., Diamond Bar, CA; Fig. 25) as described above. Mapping was performed with a saline-irrigated 3.5mm-tip catheter (Navistar Thermocool, Biosense-Webster, Inc., Fig. 25), which was used for ablation. The catheter has a locator sensor at the distal end which sends signals to the processing unit. A 3D electroanatomic map of any cardiac chamber of interest can be created with the catheter using point-by-point mapping. Additionally, the local electrograms at each point can be gated to a preselected reference electrogram to create activation or propagation color-coded maps as well as a voltage map that can be superimposed on the anatomical map of the chamber; thus a 3D electroanatomic map of the LA was

constructed by sequential acquisition of points in 3D space (Fig. 26, 27). The catheter was placed 2-4cm into each PV and slowly pulled back. Along pullback, multiple locations were recorded to tag the vein. Separate maps were built for the LA and the PVs. Pulmonary vein ostia were identified by fluoroscopic visualization of the catheter tip entering the cardiac silhouette with simultaneous impedance decrease and appearance of atrial potentials [13] [6]. The CARTO map was gated to the coronary sinus electrogram in patients who were in sinus rhythm or atrially paced during the procedure and to QRS in patients who were in AF, given its stability and prominent atrial signals.

### 3.2.2 Intra-procedure 3D-ATG and 3D reconstruction of LA and PVs

Details of rotational angiography and 3D reconstruction of LA and PVs were already described in Part I (page 11-12).

The registration process was completely automated and the overlay accuracy was evaluated by the following methods [52]: (1) the ablation catheter was able to be accurately positioned in four PVs and LA appendage in the navigation of the registered 3D-ATG; (2) a caudal drop of the catheter when withdrawing from a PV to the LA in the navigation of the registered 3D-ATG defined the PV ostium. The accuracy of the registration for PV was assessed in three projections: anterior-posterior (AP), one RAO, and one LAO view. After the final integration was performed, the real-time fluoroscopy could be shown together with semitransparent 3D-ATG overlaying. The integrated display was available to the operator during the whole procedure. The operator could observe the movement of the catheter in the registered 3D-ATG fluoroscopy image and navigate the catheter to the planned location (Fig. 28).


*Figure 25 Pictures of CARTO XP EP Navigation System (left) and NaviStar ThermoCool irrigated tip ablation catheters (right) used from Biosense Webster website.*

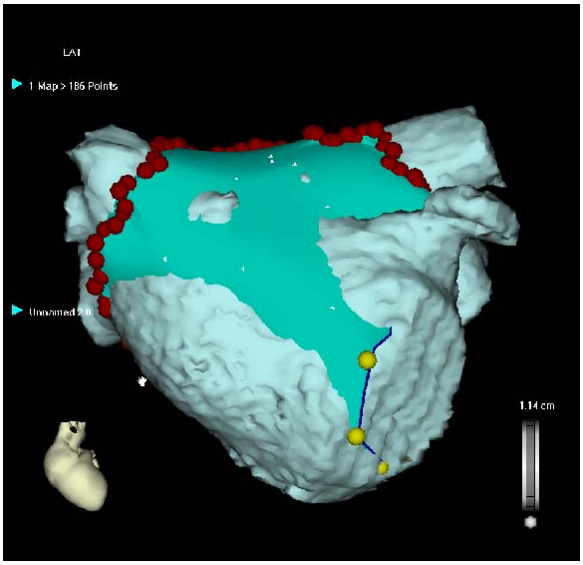


*Figure 26 CartoMerge of the left atrium-PVs isolation (anterio-posterior [AP] view)*

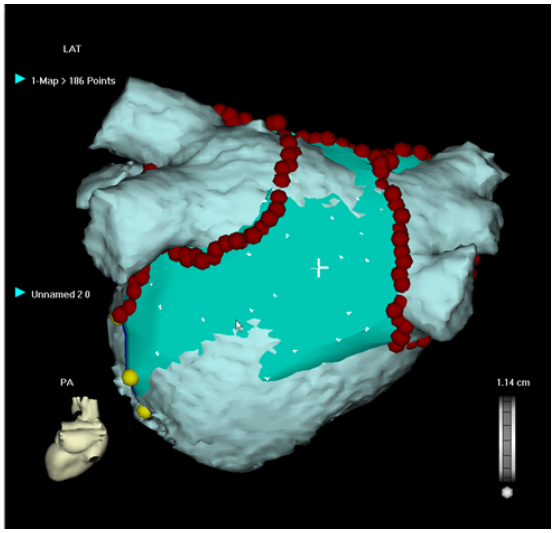


*Figure 27 CartoMerge of the left atrium-PVs isolation (postero-anterior [PA]view)*

The 3D rotational angiographic images were analyzed qualitatively in the EP reNavigator Workstation before RF ablation therapy was delivered. The classification of the datasets was based on a scale of 1-3 using the following criteria: 1='Not diagnostic': not all PV ostia are visible and/or the main body of the LA is not visible, 2='Useful': all PV ostia and the main body of the LA are visible; average image quality is present with some noise and artifacts (Fig. 29), and 3='Optimal': all PVs and the LA are visible and image artifacts are minimal (Fig. 30).

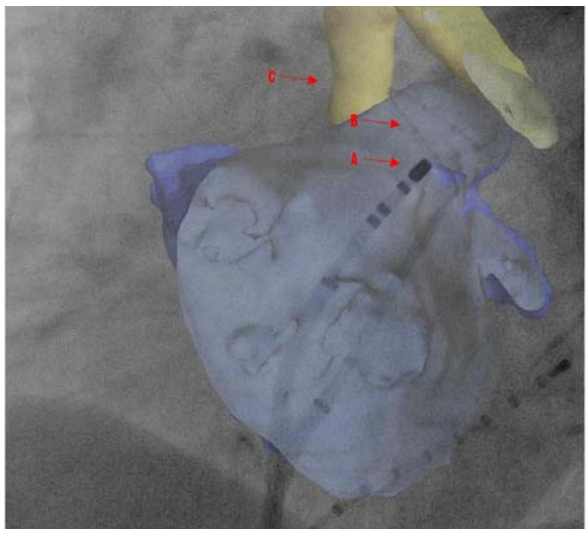


*Figure 28 The movement of catheters was observed in the registered 3D-ATG fluoroscopy image and navigated to the planned location (LAO 55°, Cran 0°).arrow A: RF ablation catheter; arrow B: circumferential mapping catheter ( lasso catheter); arrow C: bronchi.*

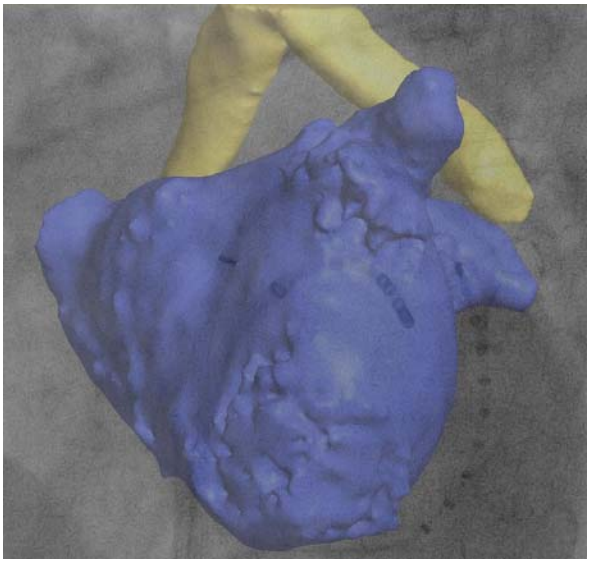

*Figure 29 The 'Useful' 3D reconstructed LA-PV image of 3D-ATG: all PV ostia and the main body of the LA are visible, average image quality is present with some noise and artifacts (LAO 48°, Cran 0°).*

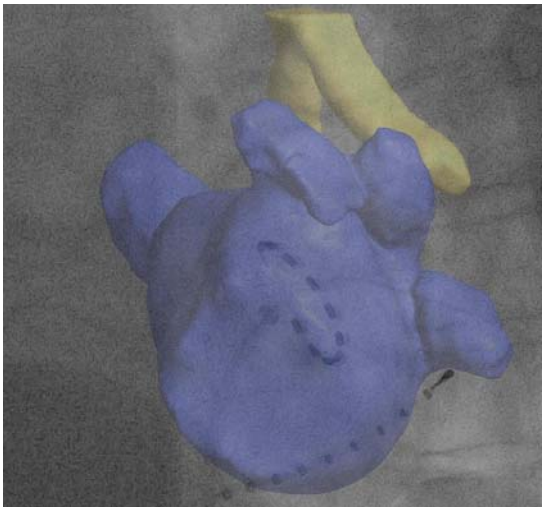

*Figure 30 The 'Optimal' 3D reconstructed LA-PV image of 3D-ATG: all PVs and the LA are visible and image artifacts are minimal (LAO 60°, Cran 0°).*

### 3.2.3 Electrophysiological study and ablation approach

Oral anticoagulation was stopped 3-7 days before the scheduled ablation and when the international normalized ratio fell below 1.8 the patient was started on low-molecular heparin subcutaneously until the day before the procedure.

During the procedure, a quadrapolar catheter (Josephson type, Bard EP, Lowell, MA, USA)

was inserted through the femoral vein and placed at a stable position on the right ventricular apex, with a pacing threshold of less than 1.5 mAm/1.0 ms. A diagnostic decapolar catheter was inserted into the coronary sinus. Two transseptal punctures were performed in order to insert an ablation catheter (Navistar, Biosense Webster, 30W energy, flow 17 ml/min) and a decapolar mapping catheter (Lasso, Biosense Webster, Diamond Bar, CA, USA) into the LA. Intravenous heparin was then administered to maintain a clotting time of 250 to 300 seconds. Sedation was applied throughout the procedure with propofol or with fentanyl and midazolam during respiratory and circulatory monitoring. The end-point of the procedure was the electrical isolation of all PVs defined as either entrance block or elimination of PV potentials at a decapolar Lasso catheter that was positioned as closely as possible to the PV ostium (Fig.15).

### 3.2.4 Radiation, procedural time analysis

Radiation exposure in 3D-ATG or CARTO was measured as dose area product (DAP) and was converted to effective dose (ED) with a standardized conversion factor of CF= 0.186 mSv $mGy^{-1}cm^{2}$.[70][71]. Procedural time for 3D-ATG was defined as the time from introduction of the angiography catheter into the LA until completion of overlay of 3D-ATG with fluoroscopy.

### 3.2.5 Follow-up

Details were seen in Part I 3.3.

### 3.2.6 Statistical analysis

Continuous variables were expressed as the mean value ± SD and compared with the one-way analysis of variance or *t*-test. A Pearson chi-square test or Fisher's exact test was used for categorical variables. Nonparametric tests were used when appropriate. Actuarial event-free rates from AF were calculated according to the Kaplan-Meier method and were compared by use of the log-rank test. *P* value <0.05 was considered statistically significant. Statistical analysis was performed using SPSS, version 17.0 (SPSS Inc.)

# 4. Results

There were 134 patients aged 59±11 years. All patients had symptomatic AF resistant to 2±1 drugs. The time since the initial diagnosis of AF to the ablation procedure was 62 months (range 1-360 months). The characteristics of the patients are presented in Table 5.

## 4.1 Procedural results

The total time for 3D-ATG imaging, segmentation, and registration was 10.1±5.0 minutes, which was shorter than with CARTO (25.4±9.1minutes, $P<0.001$). The specific radiation exposure from the 3D-ATG was also lower than with CARTO (155417.2±80487.9 vs. 32217.3±23382.9 mGy·cm$^2$; $P<0.001$) (Table 6). The global quality score for 3D-ATG was 2.3±0.9. Fifteen of the 66 reconstructed 3D-ATG images (22.7%) were scored 'useful' and 38/66 (57.6%) of these were scored 'optimal' in the procedure; all the PV ostia and LA appendages were delineated. However, in 4 patients the 3D-ATG data failed to be transferred to the EP reNavigator Workstation and were not able to be reconstructed. AF ablation was performed with the Navistar catheter after selective PV angiography in theses cases.

The mean total procedural duration was 209.5±49.8 minutes, including 50.6±23.6 minutes of fluoroscopy and 41.5±17.9 minutes of radio-frequency application. Total procedural radiation exposure was 189920.5±121945.0 mGy cm$^2$. Not only the total procedure duration and ablation time, but also the fluorotime and total procedural radiation exposure in 3D-ATG group were lower than in the CARTO group (Table 6, $P<0.05$).

Complete PV isolation was achieved in 92.4% (61/66) patients in the 3D-ATG group and 86.8% (59/68) patients in the CARTO group ($P=0.284$).

Concerning the complications, only one case of mild pericardial effusion was observed on the first postprocedural day in the CARTO group and this was absorbed in a week. No PV stenosis was observed during follow-up in either groups.

## 4.2 Follow-up

After a mean follow-up of 14±13 (IQR: 3, 24) months (14±10 months for 3D ATG vs. 15±16

for CARTO; *P*=0.739), 79/134 (59%) patients had a recurrence of AF (39/66[59.1%] of the 3D-ATG group vs. 40/68 [58.8%] of the CARTO group; *P*>0.05). There was no difference in clinical outcome using either 3D-ATG or CARTO with AF recurrence (Fig. 31). The number of patients free of AF recurrence at different follow-up points is shown in Table 7. One hundred out of 134 (74.6%) patients (52/66 [78.8%] in the 3D-ATG group vs. 48/68 [70.6%] in the CARTO group, *P*=0.275) reported symptom improvement at the end of follow-up.

Table 5. Baseline characteristics of patients who underwent ablation guided by 3D-ATG or Carto

| *Patients* | *3D-ATG* (n=66) | *Carto* (n=68) | *P* value | Total (n=134) |
|---|---|---|---|---|
| Male (%) | 33(50) | 47(69.1) | 0.024 | 80(59.7) |
| Age (y) | 60±11 | 59±10 | 0.360 | 59±11 |
| History of AF (m.) | 70±75 | 54±50 | 0.164 | 62±65 |
| Paroxysmal AF (%) | 42(63.6) | 34(50.0) | 0.111 | 76(56.7) |
| Persistent AF (%) | 24(36.4) | 34(50.0) | 0.111 | 58(43.3) |
| LVd(mm) | 49.2±4.9 | 50.8±8.0 | 0.170 | 50.0±6.6 |
| LVs(mm) | 31.9±6.2 | 35.5±10.2 | 0.023 | 33.7±8.6 |
| LA(mm) | 44.7±7.3 | 44.2±6.8 | 0.662 | 44.5±7.1 |
| LVEF, % | 63.7±9.9 | 60.1±11.8 | 0.062 | 61.9±11.0 |
| Hypertension (%) | 44(66.7) | 43(63.2) | 0.677 | 87(64.9) |
| Diabetes mellitus (%) | 9(13.6) | 6(8.8) | 0.377 | 15(22.1) |
| CAD requiring CABG or PCI (%) | 12♂(18.2) | 15(22.1) | 0.576 | 27(39.7) |
| SHD (%) | 3♂(4.5) | 3(4.4) | 0.646 | 6(8.8) |
| Cardiomyopathy (%) | 3(4.5) | 4(5.9) | 0.517 | 7(10.3) |
| VHD (%) | 2(3.0) | 6(8.8) | 0.147 | 8(11.8) |

See Table 1 for comments.

♂: 2 cases were CAD combined SHD.

Table 7. Number of patients at risk of AF recurrence

| | 1st month | 6th month* | 12th month* | 24th month* | 36th month* |
|---|---|---|---|---|---|
| 3D-ATG | 66 (100%) | 44 (66.7%) | 29 (43.9%) | 12 (18.2%) | 1 (1.5%) |
| CARTO | 68 (100%) | 28 (41.2%) | 23 (33.8%) | 19 (27.9%) | 10 (14.7%) |

* follow-up time

Table 6. Comparison between 3D-ATG group and CARTO group

| | 3D-ATG | CARTO | *P* value | total |
|---|---|---|---|---|
| Total procedural time (min.) | 185.1±35.0 | 233.1±50.8 | <0.001 | 209.5±49.8 |
| Total Fluorotime(min.) | 44.0±13.0 | 57.1±29.2 | 0.001 | 50.6±23.6 |
| Total ablation time (min.) | 34.3±15.2 | 47.0±17.9 | <0.001 | 41.5±17.9 |
| Total procedural radiation exposure (mGy.cm$^2$) | 155417.2±80487.9 | 223409.0±144649.1 | 0.001 | 189920.5±121945.0 |
| ED for procedure (mSv) | 2890.8±1497.1 | 4155.4±2690.5 | 0.001 | 3532.5±2268.2 |
| Time for 3D-ATG/CARTO mapping (min.) | 10.1±5.0 | 25.4±9.1 | <0.001 | - |
| Specific radiation exposure* (mGy.cm2) for mapping | 12108.6±1497.4 | 32217.3±23382.9 | <0.001 | - |
| ED for mapping | 225.2±27.9 | 599.2±434.9 | <0.001 | - |

min. =minutes. ED=effective dose.

*Specific radiation exposure: radiation exposure for 3D-ATG or CARTO mapping.

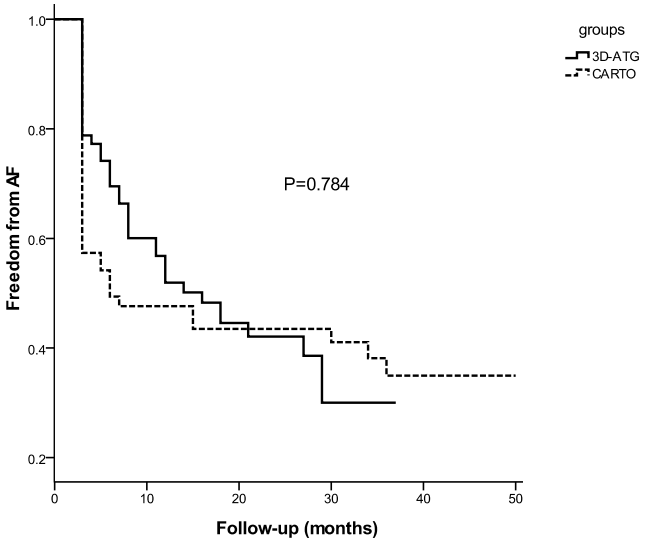


*Figure 31 Kaplan-Meier analysis of long-term atrial fibrillation-free survival in patients using 3D- ATG vs. CARTO.*

## 5. Discussion

The principle of 3D-ATG is similar to the CT scan where images acquired from different angles are reconstructed to produce a three-dimensional image. The main advantages of 3D-ATG includes more accurate representation of the left atrial anatomy, as it is performed immediately prior to the procedure and is not affected by changes in volume status of the patient between the day of imaging and the day of procedure. The radiation exposure from 3D-ATG is less than that of the CT scan [49]. However, the principle of the electroanatomic mapping system (CARTO) is that a coil placed in the magnetic field will generate an electrical current. Hence, there is a theoretical concern for increased radiation exposure of 3D-ATG in comparison to CARTO. Surprisingly, our study shows that 3D-ATG used during AF catheter ablation results in shorter procedural outcomes and shorter radiation exposure as compared with a standard 3D electroanatomical system with similar clinical outcomes. Furthermore, a recently published randomized study of 3D-ATG versus CARTO used during AF ablation reported by Knecht et al. showed that the radiation exposure, procedural times, and clinical outcomes at 10 months were similar in the two groups [68].

We utilized direct 3D-ATG with RVP in this study, and acquired a satisfactory LA reconstruction ratio (85.5% for 53 of 62 patients in whom reconstruction of LA was performed). Recent studies have shown a good correlation coefficient between 3D-ATG and cardiac computed tomography (CCT) for ostial PV diameters and LA volume at lower radiation dose and procedural costs; and the accuracy of 3D-ATG is high, irrespective of the methods used to perform 3D-ATG, which were indirect 3D-ATG (contrast injection from the right atrium or from the common trunk of the pulmonary artery), direct 3D-ATG with adenosine, direct 3D-ATG with RVP, and conventionally [55],[56]. We introduced direct ATG with RVP in the procedure of AF ablation and found good correlation in the PV ostial diameters as compared to CT imaging ($r^2$>0.85) [56].

Concerning the ablation procedure, the major findings in this study are that: (1) Rotational angiography performed with RVP method could produce a useful 3D-ATG in 85.5% cases; all the PV ostia and LA appendages could be delineated; (2) the ablation catheter could be positioned at the target point in the navigation of the registered 3D-ATG; (3) the radiation

exposure and procedural times in 3D-ATG was significantly lower or shorter than in CARTO; (4) image registration and reregistration in 3D-ATG are very convenient and accurate because the same equipment for fluoroscopy and 3D imaging is combined; (5) it is not restricted to the use of specific mapping/ablation catheters with 3D-ATG, such as Lasso/Navistar catheter for mapping/ablation, cryoballoon with ProMAP catheter, PVAC, and MESH catheter etc.

For the acute and chronic clinical outcomes, the results were similar between the two groups. For the long-term follow-up, we found a relatively higher rate of patients free from AF recurrence in 3D-ATG before and at the point of 12 months follow-up and then in the CARTO group at 24$^{th}$ month follow-up and 36$^{th}$ month follow-up without statistical difference (Table 7). Both of them were safe methods and achieved good acute success rates, but yielded high AF recurrence at long-term follow-up. Weerasooriya et al.[64] reported that the arrhythmia-free survival rates after a single catheter ablation procedure were 40%, 37%, and 29% at 1, 2, and 5 years, respectively, with most recurrences over the first 6 months; patients with long-standing persistent AF experienced a higher recurrence rate than those with paroxysmal or persistent forms. Thus, one of the explanations for our relatively lower AF-free survival rates is that the mean history of AF in our study was relatively long (62±65 months).

In comparison, CARTO provides an alternative to fluoroscopy-based systems and allows the importation of preacquired LA geometry from a CCT, MRI, or 3D-ATG for improved accuracy. Surprisingly, the use of CARTO mapping did not result in reduced radiation exposure in this study and a previous study [72]. The possible explanations may be that: (1) additional fluoroscopy is required to construct the initial map and subsequent remapping in the case of patient movement; (2) operators may not rely entirely on electroanatomical guidance and frequently use fluoroscopy to confirm catheter position.

Since contrast agents are not necessary for CARTO mapping, this method may be preferred for patients with severe heart failure, or liver and/or renal insufficiency. Another advantage of CARTO compared with 3D-ATG is that an activation map can be superimposed on the 3D anatomy, targeting sites demonstrating CFAEs during AF or facilitating diagnosis of atrial tachycardia.

This study suggests that 3D-ATG is comparable to current electroanatomical mapping system and can be used as a stand-alone imaging method to guide AF ablation applied for

different ablation catheters. Furthermore, it optimizes the clinical utilization of new catheter ablation techniques of atrial fibrillation.

Limitations

No comparison between 3D-ATG and CT was performed in this study. However, as already demonstrated elsewhere [47], [52], radiation exposure is significantly reduced with 3D-ATG as compared with a CT scan.

# 6. Conclusion

1. Simplified cryoballoon technique, PVAC, and the MESH catheter all represent safe, efficacious alternatives for PV isolation. They all reduce both procedure and fluoroscopy time and make the procedure simple. The short- and middle-term efficacy of these catheters is comparable to that of a conventional point-by-point ablation technique.

2. Three-dimensional ATG allows AF ablation to be guided with lower radiation exposure, shorter procedure time and similar outcome compared with CARTO. The ease of use and accurate 3D representation of the LA anatomy make 3D-ATG a reasonable alternative to conventional 3D electroanatomic mapping systems; however it is without advanced mapping functions.

# References

1. Schmitt C, Zrenner DB (Eds.). Catheter ablation of cardiac arrhythmias: A pratical approach. In: Deisenhofer I, Estner H, Pustowort A. Catheter ablation of atrial fibrillation. Springer, Germany: Steinkopff Verlag Darmstadt 2006: 211.
2. Wyse DG, Waldo AL, DiMarco JP, et al. A comparison of rate control and rhythm control in patients with atrial fibrillation. N Engl J Med 2002; 347: 1825-1833.
3. Takahashi A. Catheter ablation is established as a treatment option for atrial fibrillation-Is catheter ablation established as a treatment option of atrial fibrillation? (Pro)-. Circ J 2010; 74:1972-1977.
4. Moe GK, Abildskov JA. Atrial fibrillation as a self-sustaining arrhythmia independent of focal discharges. Am Heart J 1959; 58: 59-70.
5. Haïssaguerre M., Jaïs P., Shah D.C., et al. Spontaneous initiation of atrial fibrillation by ectopic beats originating in the pulmonary veins. The New England Journal of Medicine, 1998; 339:659-666.
6. Gerstenfeld E.P. Persistent pulmonary vein isolation: The elusive goal of atrial fibrillation ablation. Journal of Cardiovascular Electrophysiology. 2007;18: 392-398.
7. Di Biase L., Elayi C.S., Fahmy TS, et al. Atrial fibrillation ablation strategies for paroxysmal patients: Randomized comparison between different techniques. Circulation: Arrhythmia and Electrophysiology 2009; 2:113-119.
8. Takahashi Y., O'neill M.,D., Jönsson A, et al. How to interpret and identify pulmonary vein recordings with the lasso catheter. Heart Rhythm 2006; 3: 748-750.
9. Wright M, Haïssaguerre M., Knecht S., et al. State of the art: Catheter ablation of atrial fibrillation. Journal of Cardiovascular Electrophysiology 2008; 19: 583-592.
10. Calkins H, Brugada J, Packer DL, Cappato R, Chen S, Crijns HJ, et al. HRS/EHRA/ECAS expert consensus statement on catheter and surgical ablation of atrial fibrillation: recommendations for personnel, policy, procedures and follow-up. A report of the Heart Rhythm Society (HRS) Task Force on Catheter and Surgical Ablation of Atrial Fibrillation developed in partnership with the European Heart Rhythm Association (EHRA) and the

European Cardiac Arrhythmia Society (ECAS); in collaboration with the American College of Cardiology (ACC), American Heart Association (AHA), and the Society of Thoracic Surgeons (STS). Endorsed and approved by the governing bodies of the American College of Cardiology, the American Heart Association, the European Cardiac Arrhythmia Society, the European Heart Rhythm Association, the Society of Thoracic Surgeons, and the Heart Rhythm Society. *Europace* 2007; 9:335-79.

11. Camm AJ, Kirchhof P, Lip GY, Schotten U, Savelieva I, Van Gelder IC, et al. Guidelines for the management of atrial fibrillation: the Task Force for the Management of Atrial Fibrillation of the European Society of Cardiology (ESC). *Europace* 2010; 12:1360-1420.
12. Wann LS, Curtis AB, January CT, Ellenbogen KA, Lowe JE, Estes JA 3rd, et al. 2011 ACCF/AHA/HRS focused update on the management of patients with atrial fibrillation (Updating the 2006 Guideline): a report of the American College of Cardiology Foundation/American Heart Association Task Force on Practice Guidelines. *Heart Rhythm* 2011; 8: 157-176.
13. Pappone C, Rosanio S, Oreto G, et al. Circumferential radio-frequency ablation of pulmonary vein ostia: a new anatomic approach for curing atrial fibrillation. Circulation 2000; 102: 2619-2628.
14. Haïssaguerre M., Shah DC, Jaïs P., et al. Mapping-guided ablation of pulmonary veins to cure atrial fibrillation. Am J Cardiol 2000; 86: K9-K19.
15. Swartz JF, Pellersels G, SilversJ, et al. A catheter based curative approach to atrial fibrillation. Circulation 1994; 90(Suppl.I): I-335[abstract].
16. Nademanee K, Lockwood E, Oketani N, et al. Catheter ablation of atrial fibrillation guided by complex fractionated atrial electrogram mapping of atrial fibrillation substrate. J Cardiol 2010; 55:1-12.
17. Haïssaguerre M., Shah DC, Jaïs P., et al. Electrophysiological breakthroughs from the left atrium to the pulmonary veins. Circulation 2000; 102:2463-2465.
18. Marrouche NF, Dresing T, Cole C, et al. Circular mapping and ablation of the pulmonary vein for treatment of atrial fibrillation: impact of different catheter technologies. J Am Coll Cardiol 2002; 40:464-74.
19 Ouyang F, Bänsch D, Kuck K, et al. Complete isolation of left atrium surrounding the

pulmonary veins: New insights from the double-Lasso technique in paroxysmal atrial fibrillation. Circulation 2004; 110: 2090-2096.

20. Pappone C, Oreto G, Lamberti F, et al. Catheter ablation of paroxysmal atrial fibrillation using a 3D mapping system. Circualtion 1999; 100: 1203-8.
21. Shah D. Pulmonary vein isolation with the pulmonary vein ablation catheter (PVAC): is there a price to pay for a 'simpler', shorter procedure? Europace 2010; 12: 455-457.
22. Maan A, Shaikh AY, Mansour M, et al. Complications from catheter ablation of atrial fibrillation: A systematic review. Crit Pathways in Cardiol 2011; 10: 76-83.
23. Cappato R, Calkins H, Chen SA, et al. Updated worldwide survey on the methods, efficacy, and safety of catheter ablation for human atrial fibrillation. Circ Arrhythm Electrophysiol 2010; 3: 32-38.
24. Wazni O, Wilkoff B, Saliba W. Catheter ablation for atrial fibrillation. N Engl J Med 2011; 365: 2296-2304.
25. Ernst S. The future of atrial fibrillation ablation: new technologies and indications: atrial fibrillation. Heart 2009; 95: 158-163.
26. Andrade JG, Khairy P, Guerra PG, et al. Efficacy and safety of cryoballoon ablation for atrial fibrillation: A systematic review of published studies. Heart Rhythm 2011; 8:1444-1451.
27. Tse HF, Reek S, Timmermans C, et al. Pulmonary vein isolation using transvenous catheter cryoablation for treatment of atrial fibrillation without risk of pulmonary vein stenosis. J Am Coll Cardiol 2003; 42: 752-758.
28. Ripley KL, Gage AA, Olsen DB, et al. Time course of esophageal lesions after catheter ablation with cryothermal and radio-frequency ablation: implication for atrio-esophageal fistula formation after catheter ablation for atrial fibrillation. J Cardiovasc Electrophysiol 2007; 18: 642-646.
29. Khairy P, Chauvet P, Lehmann J, et al. Lower incidence of thrombus formation with cryoenergy versus radio-frequency catheter ablation. Circulation 2003; 107: 2045-2050.
30. Neumann T, Vogt J, Schumacher B, et al. Circumferential pulmonary vein isolation with the cryoballoon technique results from a prospective 3-center study. J Am Coll Cardiol 2008; 52:273-278.
31. Packer DL, Irwin Jm, Ruskin JN, et al. Cryoballoon ablation of pulmonary veins for

paroxysmal atrial fibrillation: first results of the North American Arctic from STOP-AF Pivotal trial. ACC 2010, March 15, Atlanta. assets. cardiosource.com/packer_stop_af1.ppt.

32. Kojodjojo P, O'Neill MD, Lim PB, et al. Pulmonary venous isolation by antral ablation with a large cryoballoon for treatment of paroxysmal and persistent atrial fibrillation:medium-term outcomes and non-randomised comparison with pulmonary venous isolation by radio-frequency ablation. Heart 2010; 96:1379-1384.
33. Van Belle Y, Janse P, Theuns D, Szili-Torok T, Jordaens L. One year follow-up after cryoballoon isolation of the pulmonary veins in patients with paroxysmal atrial fibrillation. Europace 2008;10:1271-1276.
34. Chun K.R.J., Fürnkranz A, Metzner A, Schmidt B, Tilz R, Zerm T, et al. Cryoballoon pulmonary vein isolation with real-time recordings from the pulmonary veins. J Cardiovasc Electrophysiol, 2009, 20(11): 1203-1210.
35. Tang M, Kriatselis C, Nedios S, et al. A novel cryoballoon technique for mapping and isolating pulmonary veins: A feasibility and efficacy study. J Cardiovasc Electrophysiol, 2010, 21(6): 626-631.
36. Boersma L, Wijiffels M, Oral H, et al. Pulmonary vein isolation by duty-cycled bipolar and unipolar radio-frequency energy with a multielectrode ablation catheter. Heart Rhythm 2008; 5: 1635-1642.
37. Fredersdorf S, Weber S, Jilek C, et al. Safe and rapid isolation of pulmonary veins using a novel circular ablation catheter and duty-cycled RF generator. J Cardiovasc Electrophysiol, 2009; 20(10): 1097-1101.
38. Wieczorek M, Hoeltgen R, Brueck M, et al. Pulmonary vein isolation by duty-cycled bipolar and unipolar antrum ablation using a novel multielectrode ablation catheter system: first clinical results. J Interv Card Electrophysiol 2010; 27:23-31.
39. Duytschaever M, Anne W, Papiashvili G, Vandekerckhove Y, Tavernier R. Mapping and isolation of the pulmonary veins using the PVAC catheter. Pacing and Clinical Electrophysiology 2010; 33: 168-178.
40. Beukema RP, Beukema WP, Smit JJ, Ramdat Misier AR, Delnoij PP, Wellens H, Elvan A. Efficacy of multi-electrode duty-cycled radio-frequency ablation for pulmonary vein disconnection in patients with paroxysmal and persistent atrial fibrillation. Europace, 2010;

12:502-507.

41. de Greef Y, Stockman D, Duytschaever M, et al. Initial experience with the high-density mesh ablation catheter for pulmonary vein isolation. PACE 2009; 32: 1286-1293.
42. Arruda MS, He DS, Friedman P, et al. A novel mesh electrode catheter for mapping and radio-frequency delivery at the left atrium-pulmonary vein junction: A single-catheter approach to pulmonary vein antrum isolation. J Cardiovasc Electrophysiol 2007; 18: 206-211.
43. Steinwender C., Hönig, S., Leisch F., et al. One-year follow-up after pulmonary vein isolation using a single mesh catheter in patients with paroxysmal atrial fibrillation. Heart Rhythm 2010; 7: 333-339.
44. Maagh P, van Bracht M, Butz T, et al. Eighteen months follow-up of the clinical efficacy of the high density mesh ablator (HDMA) in patients with atrial fibrillation after pulmonary vein isolation. J Interv Card Electrophysiol 2010; 29: 43-52.
45. Greef YD, Tavernier R, Duytschaever M, et al. Pulmonary vein isolation with the 30 and 35 mm high-density mesh ablator. Europace 2010; 12: 1428-1434.
46. Pratola C, Notarsefano P, Artale P, et al. Radio-frequency ablation of paroxysmal atrial fibrillation by mesh catheter. J Interv Card Electrophysiol 2009; 25: 135-140.
47. Natale A, Jalife J (Eds.). Atrial fibrillation: from bench to bedside. In: Oral H, Morady F. Integrative approaches to imaging: Fluoroscopy, CT, MRI, Echocardiography, and three-dimensional electroanatomical and noncontact mapping. Humana Press, Totowa, NJ, USA, 2008: 349.
48. Schmitt C, Zrenner DB (Eds.). Catheter ablation of cardiac arrhythmias: A practical approach. In: Ndrepepa C. Three-dimensional electroanatomic mapping systems. Springer, Germany: Steinkopff Verlag Darmstadt 2006: 58-63.
49. Kabra R, Singh J. Recent trends in imaging for atrial fibrillation ablation. Indian Pacing Electrophysiol J 2010; 10(5): 215-27.
50. Orlov M.V., Hoffmeister P, Chaudhry GM, et al. Three-dimensional rotational angiography of the left atrium and esophagus: a virtual computed tomography scan in the electrophysiology lab? Heart Rhythm 2007; 4: 37-43.
51. Thiagalingam A, Manzke R., D'Avilla A, et al. Intraprocedural volume imaging of the left

atrium and pulmonary veins with rotational X-ray angiography: implications for catheter ablation of atrial fibrillation. J Cardiovasc Electrohphysiol 2008; 19:293-300.

52. Tang M, Kriatselis C, Ye G, et al. Reconstructing and registering three-dimensional rotational angiogram of left atrium during ablation of atrial ibrillation. PACE 2009; 32: 1407-1416.
53. Li JH, Haim M, Movassaghi B. Segmentation and registration of three-dimensional rotational angiogram on live fluoroscopy to guide atrial fibrillation ablation: A new online imaging tool. Heart Rhythm 2009; 6: 231-237.
54. Sra J, Krum D, Malloy A, et al. Registration of three-dimensional left atrial computed tomographic images with projection images obtained using fluoroscopy. Circulation 2005; 112: 3763-3768.
55. Kriatselis C, Tang M, Roser M, et al. A new approach for contrast-enhanced X-ray imaging of the left atrium and pulmonary veins for atrial fibrillation ablation: rotational angiography during adenosine-induced asystole. Europace 2009; 11: 35-41.
56. Gerds-Li JH, Tang M, Kriatselis C, et al. Rapid ventricular pacing to optimize rotational angiography in atrial fibrillation. J Interv Card Electrophysiol 2009; 26: 101-107.
57. Kriatselis C, Nedios S, Orlov M, et al. Intraprocedural imaging of left atrium and pulmonary veins: A comparison study between rotational angiography and cardiac computed tomography. PACE 2011; 34: 315-322.
58. Kriatselis C, Tang M, Nedios S, et al. Intraprocedural reconstruction of the left atrium and pulmonary veins as a single navigation tool for ablation of atrial fibrillation: a feasibility, efficacy, and safety study. Heart Rhythm 2009; 6: 733-741.
59. Wijffels MCEF, Van Oosterhout MF, Vos MA, JD, et al. Characterization of lesions in swine atrium using novel multielectrode ablation catheters. Eru Heart J 2008; 29 (Abstract Suppl): 412[P2632].
60. Nault I, Miyazaki S, Forclaz A, et al. Drugs vs. ablation for the treatment of atrial fibrillation: the evidence supporting catheter ablation. Eur Heart J 2010; 31: 1046-1054.
61. Hofmann R, Hönig S, Leisch F, et al. Pulmonary vein isolation with mesh Ablator versus Cryoballoon catheters: 6-month outcomes. J Interv Card Electrophysiol 2010; 29: 179-185.
62. Bulava A, Haniš J, Sitek D, et al. Catheter ablation for paroxysmal atrial fibrillation: A

randomized comparison between multielectrode catheter and point-by-point ablation. PACE 2010; 33:1039-1046.

63. Duytschaever M, Anne W, Papiashvili G, et al. Mapping and isolation of the pulmonary veins using the PVAC catheter. PACE 2010; 33: 168-178.
64. Weerasooriya R, Khairy P, Litalien J, et al. Catheter ablation for atrial fibrillation: Are results maintained at 5 years of follow-up? J. Am. Coll. Cardiol. 2011; 57:160-166.
65. Mansour M, Ferleo GB, Pappalardo A, et al. Initial experience with the mesh catheter for pulmonary vein isolation in patients with paroxysmal atrial fibrillation. Heart Rhythm 2008; 5: 1510-1516.
66. Pappalardo A, Forleo GB, Avella A, et al. Acute and long term results of pulmonary v;ein isolation with the mesh catheter for paroxysmal atrial fibrillation (abstr.). Europace 2009; 11: 421.
67. Kojodjojo P, MBBS, Davies W, et al. How to perform antral pulmonary venous isolation using the cryoballoon. Heart Rhythm 2011; 8:1452-1456.
68. Kim YH. Cryoballoon approach for atrial fibrillation ablation: free from complications? J Cardiovasc Electrophysiol 2010; 21: 875-876.
69. Khaykin Y, Oosthuizen R, Zarnett L, et al. CARTO-guided vs. NavX-guided pulmonary vein antrum isolation and pulmonary vein antrum isolation performed without 3-D mapping: effect of the 3-D mapping system on procedure duration and fluoroscopy time. J Interv Card Electrophysiol 2011; 30: 233-240.
70. Ector J, Dragusin O, Adriaenssens B, et al. Obesity is a major determinant of radiation dose in patients undergoing pulmonary vein isolation for atrial fibrillation. J Am Coll Cardiol 2007; 50: 234-242.
71. Schultz FW, Zoetelief J. Dose conversion coefficients for interventional procedures. Radiat Prot Dosimetry 2005; 117: 225-230.
72 Knecht S, Wright M, Akrivakis S, et al. Prospective randomized comparison between the conventional electroanatomical system and three-dimensional rotational angiography during catheter ablation for atrial fibrillation. Heart Rhythm 2010; 7: 459-465.

# Abbreviations

AF= atrial fibrillation

AP= anterior-posterior

ATG= rotational atriography

AV= atrioventricular

CABG= coronary artery bypass graft

CAD= coronary artery disease

CARTO= magnetic electroanatomical mapping system

CCT= cardiac computed tomography

CF= conversion factor

CFAEs= complex atrial fractionated electrograms

95% CI= 95% confidence interval

CPVA= circumferential pulmonary vein ablation

CS= coronary sinus

CT= computed tomography

3D= three-dimensional

DAP= dose area product

ED= effective dose

EP= electrophysiology

INR= international normalized ratio

IQR= interquartile range

LA= left atrium

LAA= left atrial appendage

LAO= left anterior oblique

LCPV= left common pulmonary vein

LIPV= left inferior pulmonary vein

LSPV= left superior pulmonary vein

LVd= left ventricular end-diastolic diameter

LVs= left ventricular end-systolic diameter

LVEF= left ventricular ejection fraction

MESH= high-density mesh ablation catheter

MRI= magnetic resonance imaging

PAF= paroxysmal atrial fibrillation

PCI= percutaneous coronary intervention

PNP= phrenic nerve palsy

PVAC= pulmonary vein ablation catheter

PV= pulmonary vein

PVI= pulmonary vein isolation

RA= right atrium

RAO= right anterior oblique

RF= radio frequency

RIPV= right inferior pulmonary vein

RMPV= right middle pulmonary vein

RR= relative risk

RSPV= right superior pulmonary vein

ATG= rotational angiography

RVA= right ventricular apex

RVP= rapid ventricular pacing

SD= standard deviation

SHD=structural heart disease

VHD= valvular heart disease

DAP= radiation dosis as dose area product

## Acknowledgements

I am truly grateful to Prof. Dr. Fleck for his guidance and strong support of my work in the electrophysiologic laboratory at the Deutsches Herzzentrum Berlin and to Prof. Dr. Gerds-Li for expert direction in both my research and daily clinical work and his expert editorial assistance with my dissertation!

I deeply thank Dr. Kriatselis for his selfless help with my study of electrophysiology and all colleagues in the EP laboratory for their support of my work!

Thanks to Mrs. Gale for her editorial assistance with my dissertation!

Many thanks go also to my family for their support during my more than one year's work and study in Berlin.

Xiao-Ming Chen

in Guangzhou, VR China

01.02.2012

**Erklärung**

„Ich, **Xiao-Ming Chen**, erkläre, dass ich die vorgelegte Dissertation mit dem Thema: **Techniques of Mapping and Pulmonary Vein Isolation in Patients with Atrial Fibrillation** selbst verfasst und keine anderen als die angegebenen Quellen und Hilfsmittel benutzt, ohne die (unzulässige) Hilfe Dritter verfasst und auch in Teilen keine Kopien anderer Arbeiten dargestellt habe.“

Datum 20.05.2012 Unterschrift Xiao-Ming Chen

# Curriculum vitae

**Mein Lebenslauf wird aus datenschutzrechtlichen Gründen in der elektronischen Version meiner Arbeit nicht veröffentlicht.**